U.S. DEPARTMENT OF COMMERCE
National Technical Information Service

PB-255 460

WEST VIRGINIA POWER PLANT EVALUATION

H. E. Cramer Company, Incorporated

PREPARED FOR
Environmental Protection Agency

May 1976

PB 255 460

REPRODUCED BY
NATIONAL TECHNICAL
INFORMATION SERVICE
U.S. DEPARTMENT OF COMMERCE
SPRINGFIELD, VA. 22161

BIBLIOGRAPHIC DATA SHEET	1. Report No. EPA 903/9-75-022 .	2.	3. Recipient's Accession No.

4. Title and Subtitle
West Virginia Power Plant Evaluation

5. Report Date
May 1976

6.

7. Author(s)
H. E. Cramer J. F. Bowers, Jr.

8. Performing Organization Rept. No.

9. Performing Organization Name and Address
H. E. Cramer Company Inc.
540 Arapeen Drive
Salt Lake City, Utah 84108

10. Project/Task/Work Unit No.

11. Contract/Grant No.

12. Sponsoring Organization Name and Address
U. S. Environmental Protection Agency
Region III
Philadelphia, Penna 19106 .

13. Type of Report & Period Covered

14.

15. Supplementary Notes

16. Abstracts
Using a Gaussian diffusion model, calculations of the effects of the Mitchell and Kammer power plants on ambient air quality are made. The highest predicted 24 hour average SO_2 level is 1219 $\mu g/m^3$. Comparisons between model calculations and measurments made by EPA's Las Vegas laboratory are shown. Excellent agreement is shown for plume rise, axial concentration, and ground level concentration.

17. Key Words and Document Analysis. 17a. Descriptors
Power plants
Sulfur Dioxide
Models
Model Validation

17b. Identifiers/Open-Ended Terms

17c. COSATI Field/Group

PRICES SUBJECT TO CHANGE

18. Availability Statement	19. Security Class (This Report) UNCLASSIFIED	21. No. of Pages 104
i	20. Security Class (This Page) UNCLASSIFIED	22. Price $5.50

EPA 903/9-75-022

WEST VIRGINIA POWER PLANT EVALUATION

Prepared By

H. E. Cramer and J. F. Bowers, Jr.

Prepared For

U. S. Environmental Protection Agency
Region III
Philadelphia, Pennsylvania 19106

May 1976

H. E. Cramer company, inc.
540 ARAPEEN DRIVE
UNIVERSITY OF UTAH RESEARCH PARK
SALT LAKE CITY, UTAH 84108

ACKNOWLEDGEMENTS

We are especially indebted to Dr. Peter Finkelstein, EPA Region III Meteorologist and our Project Officer, for his guidance and assistance during this study. Also, we wish to thank Mr. E. Klappenbach, EPA Region V Meteorologist, and Mr. S. Smallwood of the Wheeling Office of the West Virginia Air Pollution Control Commission for their assistance in obtaining emissions data for the major SO_2 sources in the vicinity of the Mitchell and Kammer Power Plants.

The field measurement program conducted by the EPA Environmental Monitoring and Support Laboratory (Las Vegas, Nevada) provided a unique data set to test the diffusion-modeling techniques used in this study. We wish to thank Mr. F. Johnson, Mr. R. Evans and Mr. T. Zeller of EMSL for providing us with the airborne SO_2 concentration measurments discussed in Appendix C.

TABLE OF CONTENTS

Section	Title	Page No.
1	INTRODUCTION	1
2	1.1 Background	1
	1.2 Purpose and Approach	1
	1.3 Special EPA Observations	3
	1.4 Report Organization	4
2	SOURCE AND METEOROLOGICAL INPUT PARAMETERS	6
	2.1 Source Input Parameters	6
	2.2 Meteorological Input Parameters	9
3	CALCULATION PROCEDURES AND RESULTS	21
	3.1 Maximum 3-Hour and 24-Hour Ground-Level SO_2 Concentrations Produced by Emissions from the Mitchell and Kammer Power Plants	21
	3.2 Effects of the Interaction of the Kammer, Mitchell and Burger Plumes on Short-Term Maximum Ground-Level Concentrations	27
	3.3 Annual Average SO_2 Concentrations Produced by Emissions from the Mitchell and Kammer Power Plants	35
4	SUMMARY OF RESULTS	42
	4.1 Calculated Maximum Short-Term Concentrations	42
	4.2 Calculated Maximum Annual Concentrations	48
REFERENCES		53
Appendix		
A	MATHEMATICAL MODELS USED TO CALCULATE GROUND-LEVEL CONCENTRATIONS	A-1
	A.1 Introduction	A-1
	A.2 Plume-Rise Formulas	A-3
	A.3 Short-Term Concentration Model	A-4
	A.4 Long-Term Concentration Model	A-13
	A.5 Application of the Short-Term and Long-Term Concentration Models in Complex Terrain	A-18

TABLE OF CONTENTS (continued)

Appendix	Title	Page No.
B	ANNUAL FREQUENCY DISTRIBUTION OF WIND SPEED AND WIND DIRECTION AT THE GREATER PITTSBURGH AIRPORT	B-1
C	COMPARISON OF CALCULATED AND OBSERVED PLUME CHARACTERISTICS FOR THE MITCHELL AND KAMMER POWER PLANTS	C-1
	C.1 Background	C-1
	C.2 Emissions Data for the EMSL Trials	C-2
	C.3 Meteorological Data for the EMSL Trials	C-2
	C.4 Results of the Analysis	C-5
	C.5 Conclusions	C-13

SECTION 1
INTRODUCTION

1.1 BACKGROUND

The U. S. Environmental Protection Agency, Region III is evaluating the impact on ambient air quality of SO_2 emissions from the Kammer and Mitchell coal-fired eletrical generating plants, located in Marshall County, West Virginia. The two power plants are situated approximately two kilometers apart on the east side of the Ohio River Valley in the northern panhandle of West Virginia about 40 kilometers south of Wheeling. As shown in Figure 1-1, which is a topographic map of the area surrounding the plant sites, the Ohio River Valley has an approximate north-south orientation in this area. The valley width varies from about one to two kilometers and the average elevation of the valley floor on which the plant sites are located is about 200 meters (650 feet) above sea level. Terrain elevations on both sides of the Ohio River Valley, for distances of at least 20 kilometers away from the river, range from 300 to 400 meters (1,000 to 1,300 feet) above sea level except where creeks and small streams have made deep cuts. It follows that the stack plumes from both the Kammer and Mitchell Power Plants, when they are brought to the ground by turbulent mixing and other meteorological processes, will almost always interact with terrain elevations that are 150 to 200 meters above the plant-grade elevations.

1.2 PURPOSE AND APPROACH

The purpose of this report is to provide EPA, Region III with diffusion-model estimates of the short-term and long-term ground-level SO_2 concentrations produced by the stack emissions from both the Kammer and Mitchell Power Plants. Short-term maximum concentration estimates have been made for Kammer and

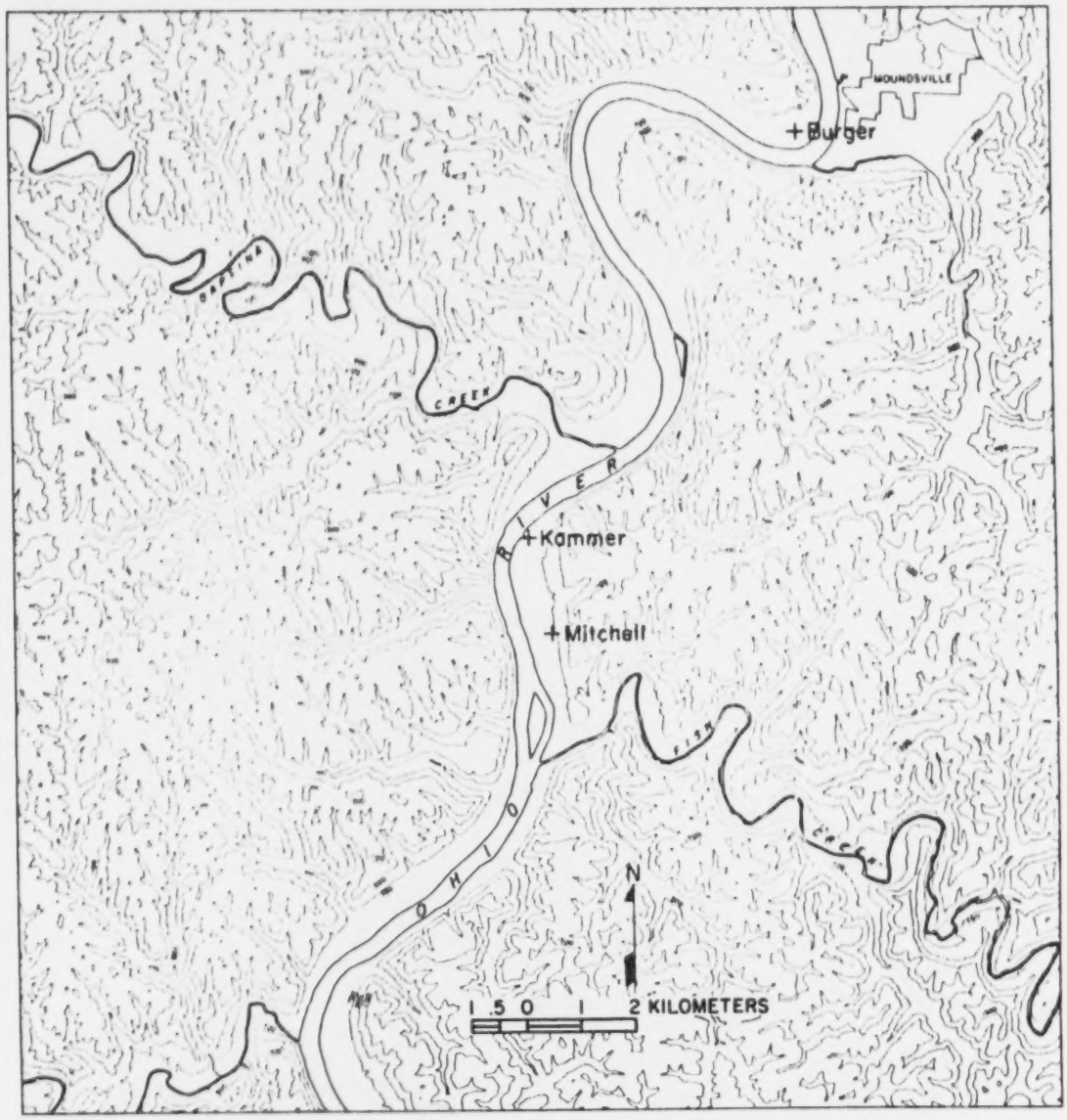

FIGURE 1-1. Topographic map of the area surrounding the Mitchell and Kammer Power Plants. Elevations are in feet above mean sea level and the contour interval is 200 feet (61 meters). The + symbols show the locations of the Mitchell and Kammer Power Plants as well as the Berger Plant which is the only other major SO_2 source in the area.

Mitchell individually and for the combined effects of Kammer, Mitchell and the other major SO_2 source in the area, the Burger Power Plant, which is located about 10 kilometers north northeast of Kammer and Mitchell (see Figure 1-1).

The diffusion models used to calculate the SO_2 ground-level concentrations presented in this report are advanced forms of Gaussian-plume equations that provide for the effects of buoyant plume rise, variations in terrain elevation and wind persistence. These diffusion models have been successfully used to calculate ground-level SO_2 concentration patterns produced by the major SO_2 stationary sources in Allegheny County, Pennsylvania in recent work for EPA, Region III (Cramer, Geary and Bowers, 1975). The terrain and meteorology of the Allegheny County area and the area surrounding the Kammer and Mitchell Power Plants are quite similar. For this reason and because the Greater Pittsburgh Airport was the closest site to the two power plants for which the requisite meteorological data were available, the general meteorological model inputs used in the Allegheny County calculations, as well as the annual wind distributions and mixing depth data for the Greater Pittsburgh Airport, were used in this study.

1.3 SPECIAL EPA OBSERVATION PROGRAM

During late August and early September 1975, the EPA Environmental Monitoring and Support Laboratory (EMSL) made a series of special measurements of the characteristics of the plumes from the Mitchell and Kammer Power Plants (Johnson, et al, 1976). As discussed in detail in Appendix C, the EMSL measurements were used to check the accuracy of the diffusion-modeling techniques used in this report. The average of the ratios of calculated and observed plume rises for Mitchell, Kammer No. 1 and Kammer No. 2 are 1.04, 0.97 and 1.24, respectively. As explained in Appendix C, the observed plume rises for Kammer No. 2 are lower than the actual plume rises because of the effects of reflection from the terrain at the measurement distances. Thus, the average ratio of calculated

and actual plume rises for Kammer No. 2 is likely close to unity as are the average ratios for Mitchell and Kammer No. 1. At downwind distances on the order of 4 kilometers, the average of the ratios of calculated and observed axial concentrations is 1.21. Bifurcation of the Mitchell plume during several trials and the time lag of the EMSL airborne SO_2 measurement system may largely account for this difference. At distances of 10 kilometers or more from the stacks, the average of the ratios of calculated and observed axial concentrations is 0.70. Background SO_2 concentration levels measured by the EMSL helicopter ranged from about 0.01 to 0.05 parts per million (25 to 130 micrograms per cubic meter). The fact that the calculated values do not include any background may explain the tendency of the model to underestimate axial concentrations at long downwind distances. On two occasions when the Kammer stack plumes were observed to be impacting on elevated terrain the EMSL helicopter made a number of passes through the plumes at a height of 15 to 30 meters above ground level. The average of the ratios of calculated and observed short-term ground-level concentrations is 1.20 if terrain effects are included and 0.40 if they are excluded and it is assumed that the plume axes follow the terrain. We conclude that the EMSL measurements show that the short-term modeling techniques used in this study are valid for averaging times of 1 hour or less.

1.4 REPORT ORGANIZATION

The source and meteorological inputs used in the diffusion-model calculations are described in Section 2. The calculation procedures and the detailed results of the calculations are given in Section 3. The results of the calculations are summarized in Section 4 and estimates are presented of the impact of the Kammer and Mitchell Power Plants on both long-term and short-term ambient air quality. The short-term and long-term atmospheric diffusion models used to make the calculations are described in detail in Appendix A. The annual frequency distribution of wind speed and wind direction at the Greater Pittsburgh Airport, classified according to the Pasquill stability categories and used in the annual calculations, is

presented in Appendix B. Appendix C compares airborne measurements of the short-term characteristics of the Mitchell and Kammer plumes with the characteristics predicted by the short-term diffusion model used in this study.

SECTION 2

SOURCE AND METEOROLOGICAL INPUT PARAMETERS

2.1 SOURCE INPUT PARAMETERS

Table 2-1 lists the stack and emissions data for the Kammer and Mitchell Power Plants supplied by EPA, Region III. The SO_2 emissions rates in the table assume that both plants are operating at capacity and the sulfur content of the coal burned by the Mitchell plant is 3.6 percent while the sulfur content of the coal burned by the Kammer plant is 4.1 percent. The Universal Transverse Mercator (UTM) coordinates for the locations of the two power plants are also listed in the table. The stack and emissions data in Table 2-2 are for the other major SO_2 source in the area, the Burger Power Plant, and were provided by the West Virginia Air Pollution Control Commission.

It should be noted that the Kammer and Mitchell Power Plants have unusually high stack exit velocities. Because the ratios of the stack exit velocities to the mean wind speed will almost always be greater than 1.5, plume downwash in the wake of the stacks should rarely if ever occur. Thus, the semi-empirical correction factor f (Equation A-3) in Appendix A), which reduces the buoyant plume rise to zero for ambient wind speeds equal to or greater than the stack exit velocity, will have no effect for these stacks. On the other hand, the exit velocity of the Burger stack is relatively low and the ratio of the stack exit velocity to the mean wind will frequently be less than 1.5 (i.e., whenever the mean wind speed is greater than 5.9 meters per second). Thus, plume downwash in the wake of the Burger stack is possible and the correction factor f will significantly reduce the calculated buoyant rise of the Burger plume and will significantly increase the calculated maximum ground-level concentrations for mean wind speeds greater than 5.9 meters per second. However, there is some question as to the strict applicability of the correction factor f for the Burger stack which cannot be

TABLE 2-1

STACK AND EMISSIONS DATA FOR THE
MITCHELL AND KAMMER POWER PLANTS

Parameter	Parameter Value		
	Mitchell	Kammer No. 1	Kammer No. 2
Stack height (m)	365.8	183.2	183.2
Stack exit temperature (^{o}K)	441.3	441.3	441.3
Stack diameter (m)	10.06	4.75	3.35
Stack exit velocity (m/sec)	30.3	34.6	34.7
SO_2 emission rate (g/sec)*	11,669.6	3,698.0	1,849.0
UTM X coordinate (m)	515,800.0	515,320.0	515,320.0
UTM Y coordinate (m)	4,408,670.0	4,410,330.0	4,410,330.0
Plant elevation (m above mean sea level)	210.0	197.0	197.0

*At rated capacity

TABLE 2-2

STACK AND EMISSIONS DATA FOR THE
BURGER POWER PLANT

Parameter	Parameter Value
Stack height (m)	259.1
Stack exit temperature (^{o}K)	446
Stack diameter (m)	6.56
Stack exit velocity (m/sec)	8.84
SO_2 emission rate (g/sec)	2,054
UTM X coordinate (m)	520,500
UTM Y coordinate (m)	4,417,500
Plant elevation (m above mean sea level)	198

satisfactorily resolved in the absence of comprehensive observations of plume behavior for mean wind speeds on the order of the stack exit velocity. According to Briggs (1969) and others, exit-velocity (downwash) restrictions on plume rise may not occur if the stack exit Froude number (see Briggs, 1969, p. 6) is less than 1.0. It has also been our experience (see Appendix D of Cramer, Bowers and Geary, 1976) that the correction factor f should not be used when the Froude number is less than 1.0 and should clearly be used when the Froude number is 3.0 or greater. Because the Froude number of the Burger stack is 2.2, the maximum ground-level SO_2 concentrations that we have calculated for the Burger Power Plant may be safe sided.

2.2 METEOROLOGICAL INPUT PARAMETERS

Meteorological inputs for the diffusion-model calculations in this report were specified following procedures identical to those used in similar diffusion-model calculations of SO_2 ground-level concentrations in Allegheny County, Pennsylvania (Cramer, Geary and Bowers, 1975). Inputs required by the long-term concentration model described in Appendix A were principally obtained from the annual distribution of wind speed and wind direction, classified according to the Pasquill stability categories, for the Greater Pittsburgh Airport during the ten-year period from January 1963 through December 1972. This annual distribution was developed from surface weather observations using the definitions of the Pasquill stability categories given by Turner (1964), which are based on solar radiation (insolation) and wind speed. Tables 2-3 and 2-4 list the parameters that define the various stability categories. The wind speeds in Table 2-3 are in knots because airport surface wind speeds are reported to the nearest knot by the National Weather Service and Turner's classification is based on this convention. The thermal stratifications represented by the various Pasquill stability categories are:

TABLE 2-3

PASQUILL STABILITY CATEGORY AS A FUNCTION OF INSOLATION AND WIND SPEED

Wind Speed (knots)	Insolation Index						
	1	3	2	1	0	-1	-2
0, 1	A	A	B	C	D	F	F
2, 3	A	B	B	C	D	F	F
4, 5	A	B	C	D	D	E	F
6	B	B	C	D	D	E	F
7	B	B	C	D	D	D	E
8, 9	B	C	C	D	D	D	E
10	C	C	D	D	D	D	E
11	C	C	D	D	D	D	D
≥12	C	D	D	D	D	D	D

TABLE 2-4

INSOLATION CATEGORIES

Insolation	Insolation Category Number
Strong	4
Moderate	3
Slight	2
Weak	1
Overcast ≤7000 feet (day or night)	0
Cloud Cover >4/10 (night)	-1
Cloud Cover ≤4/10 (night)	-2

- A--Extremely unstable
- B--Unstable
- C--Slightly unstable
- D--Neutral
- E--Slightly stable
- F--Stable

The Greater Pittsburgh Airport is located approximately 85 kilometers northeast of the Mitchell and Kammer Power Plants at an elevation of 367 meters above mean sea level, which approximately corresponds to the mean elevation of the terrain surrounding the Mitchell and Kammer Power Plants. Because the stabilization heights of the plumes from both power plants are well above the highest terrain, we believe that the wind data from the Greater Pittsburgh Airport can safely be applied, following the same procedures used in the Allegheny County SO_2 study mentioned above, to the area surrounding the Mitchell and Kammer Power Plants. The annual joint frequency distribution of wind-speed and wind-direction categories at the Greater Pittsburgh Airport, classified according to the Pasquill stability categories, is given in Appendix B. As noted in Appendix A, a wind-profile exponent law is used to adjust the mean wind speed in each wind-speed category from the measurement height at the Greater Pittsburgh Airport (6.1 meters above the airport elevation) to the stack heights for the plume-rise calculations. A similar wind-profile exponent law is used to adjust the mean wind speeds to the plume stabilization heights for the concentration calculations. Values of the wind-profile exponent p assigned to the various combinations of wind speed and stability are listed in Table 2-5. These exponents are based on the results obtained by DeMarrais (1959) and Cramer, et al. (1972).

The expression for σ_z used to calculate vertical plume expansion (see Equation (A-13) in Appendix A) in both the short-term and long-term diffusion models includes the effects of the initial vertical plume dimension and relates σ_z

TABLE 2-5

WIND PROFILE EXPONENTS

Pasquill Stability Category	Wind Speed (m/sec)					
	0-1.5	1.6-3.1	3.2-5.1	5.2-8.2	8.3-10.8	>10.8
A	0.10	0.10	----	----	----	----
B	0.15	0.10	0.10	----	----	----
C	0.20	0.15	0.10	0.10	0.10	0.10
D	0.25	0.20	0.15	0.10	0.10	0.10
E	0.30	0.25	0.20	----	----	----
F	0.35	0.30	----	----	----	----

TABLE 2-6

VERTICAL TURBULENT INTENSITIES

Pasquill Stability Category	σ_E' (radians)
A	0.1745
B	0.1080
C	0.0735
D	0.0465
E	0.0350
F	0.0235

directly to the vertical turbulent intensity or standard deviation of the vertical wind angle σ_E'. The values of σ_E' listed in Table 2-6 for the various Pasquill stability categories are based in part on the measurements of Luna and Church (1971) and on the σ_E' values implicit in the vertical expansion curves presented by Pasquill (1961).

The expression for σ_y used to calculate lateral plume expansion (see Equation (A-11) of Appendix A) in the short-term diffusion model includes the effects of the initial lateral plume dimension and relates σ_y directly to the lateral turbulent intensity or standard deviation of the azimuth wind angle σ_A'. In accord with the measurements of Luna and Church (1971) and others, we assume that σ_A' is equivalent to σ_E' for averaging times of ten minutes or less at heights $\geq$100 meters above the surface. A $t^{1/5}$ law (Osipov, 1972 and others) is used to extend the ten-minute values of σ_A' to longer averaging times.

We have analyzed seasonal tabulations of twice-daily observations of mixing depth and average surface wind speed at the Greater Pittsburgh Airport for the period 1960 through 1964 (Environmental Data Service, 1966) in order to determine seasonal median early-morning and afternoon mixing depths for each wind-speed category. The seasonal median mixing depths were then averaged to obtain annual mixing depths for each wind-speed category. The annual afternoon mixing depths were assigned to the A, B and C stability categories; the annual early morning mixing depths were assigned to the E and F stability categories; and the annual early morning and afternoon mixing depths were averaged and assigned to the D stability category. Table 2-7 gives the mixing depths for the joint combinations of wind-speed and stability categories.

Requisite inputs to the Briggs (1971) plume-rise formulas given in Section A.2 of Appendix A include the vertical potential temperature gradient and the ambient

TABLE 2-7

MIXING DEPTHS IN METERS

Pasquill Stability Category	Wind Speed (m/sec)					
	0-1.5	1.6-3.1	3.2-5.1	5.2-8.2	8.3-10.8	> 10.8
A	1248	1285	----	----	----	----
B	1248	1285	1300	----	----	----
C	1248	1285	1300	1300	1300	1300
D	698	789	991	1153	1191	1191
E	148	293	653	----	----	----
F	148	293	----	----	----	----

TABLE 2-8

VERTICAL POTENTIAL TEMPERATURE
GRADIENTS IN DEGREES KELVIN PER METER

Pasquill Stability Category	Wind Speed (m/sec)					
	0-1.5	1.6-3.1	3.2-5.1	5.2-8.2	8.3-10.8	> 10.8
A	0.000	0.000	----	----	----	----
B	0.000	0.000	0.000	----	----	----
C	0.000	0.000	0.000	0.000	0.000	0.000
D	0.015	0.010	0.005	0.003	0.003	0.003
E	0.030	0.020	0.015	----	----	----
F	0.040	0.030	----	----	----	----

air temperature. Table 2-8 lists the potential temperature gradients and Table 2-9 lists the ambient air temperatures used in the annual average concentration calculations. The potential temperature gradients in Table 2-8 are based on the Turner (1964) and Pasquill (1961) definitions of the Pasquill stability categories, the measurements of Luna and Church (1971) and our previous experience. The average of the afternoon temperatures measured at the Greater Pittsburgh Airport during the period 1963 through 1972 was assigned to the A, B and C stability categories; the average of the morning and evening temperatures was assigned to the D stability category; and the average of the nighttime temperatures was assigned to the E and F categories.

In calculating maximum 3-hour and 24-hour ground-level concentrations, wind-persistence statistics from the Greater Pittsburgh Airport have been used to guide the selection of appropriate wind speeds and wind directions. Table 2-10 shows the total number of occurrences, during the ten-year period 1963 through 1972, of the combined persistence of wind direction within each 22.5-degree sector and wind speeds above 5.1 and 8.2 meters per second for time periods equal to or greater than 12, 18 and 24 hours. Tables 2-11 and 2-12 show the total number of occurrences during the two-year period 1963 through 1964 of the 1- to 24-hour combined persistence of wind directions and mean wind speeds above 5.1 and 8.2 meters per second, respectively. The years 1963 and 1964 are the only years of record for which consecutive hourly surface observations at the Greater Pittsburgh Airport are available; for the remaining years (1965-1972), the available record contains one surface observation every three hours.

We recognize that the Greater Pittsburgh Airport wind-persistence statistics probably do not strictly apply to the area surrounding the Kammer and Mitchell Power Plants. However, the Greater Pittsburgh Airport is the closest station to the Kammer and Mitchell Power Plants for which such data were available. Also, moderate-to-strong winds that persist for 6 hours or more are generally associated with large

TABLE 2-9

AMBIENT AIR TEMPERATURES

Pasquill Stability Category	Ambient Air Temperature (^{o}K)
A	287
B	287
C	287
D	284
E	281
F	281

TABLE 2-10

TOTAL NUMBER OF OCCURRENCES OF THE COMBINED PERSISTENCE OF WIND DIRECTION AND WIND SPEED ABOVE 5.1 AND 8.2 METERS PER SECOND AT THE GREATER PITTSBURGH AIRPORT DURING THE PERIOD 1963-1972

Wind Direction	Mean Wind Speed > 5.1 m/sec			Mean Wind Speed > 8.2 m/sec		
Hours of Persistence	≥12	≥18	≥24	≥12	≥18	≥24
N	3	0	0	0	0	0
NNE	0	0	0	0	0	0
NE	0	0	0	0	0	0
ENE	2	1	0	0	0	0
E	1	0	0	0	0	0
ESE	0	0	0	0	0	0
SE	1	0	0		0	0
SSE	0	0	0	0	0	0
S	1	0	0	0	0	0
SSW	1	0	0	0	0	0
SW	10	1	0	0	0	0
WSW	32	5	4	7	1	0
W	80	18	10	13	3	3
WNW	20	5	0	2	0	0
NW	8	1	0	1	0	0
NNW	8	0	0	0	0	0

TABLE 2-11

TOTAL NUMBER OF OCCURRENCES OF THE COMBINED PERSISTENCE OF WIND DIRECTION AND WIND SPEED ABOVE 5.1 METERS PER SECOND AT THE GREATER PITTSBURGH AIRPORT FOR THE PERIOD 1963 - 1964

Number of Hours of Persistence	Wind Direction (Sector)															
	N	NNE	NE	ENE	E	ESE	SE	SSE	S	SSW	SW	WSW	W	WNW	NW	NNW
≥1	238	66	21	55	39	85	79	44	110	173	548	839	773	560	400	342
≥2	68	9	5	18	8	16	21	7	24	34	156	274	236	179	103	90
≥3	25	2	0	10	2	8	8	1	7	10	74	125	108	73	41	31
≥4	14	1	0	5	2	1	4	0	2	1	35	67	59	41	20	16
≥5	8	1	0	4	0	1	3	0	1	0	22	45	33	25	8	8
≥6	6	0	0	3	0	0	3	0	0	0	6	25	17	12	3	6
≥7	5	0	0	2	0	0	1	0	0	0	3	17	12	8	2	3
≥8	3	0	0	1	0	0	0	0	0	0	2	11	8	4	2	2
≥9	2	0	0	1	0	0	0	0	0	0	1	6	4	2	2	2
≥10	2	0	0	1	0	0	0	0	0	0	0	5	3	2	0	1
≥11	2	0	0	0	0	0	0	0	0	0	0	4	3	2	0	1
≥12	1	0	0	0	0	0	0	0	0	0	0	3	2	1	0	1
≥13	1	0	0	0	0	0	0	0	0	0	0	2	2	1	0	1
≥14	1	0	0	0	0	0	0	0	0	0	0	2	0	1	0	0
≥15	0	0	0	0	0	0	0	0	0	0	0	2	0	0	0	0
≥16	0	0	0	0	0	0	0	0	0	0	0	2	0	0	0	0
≥17	0	0	0	0	0	0	0	0	0	0	0	1	0	0	0	0
≥18	0	0	0	0	0	0	0	0	0	0	0	1	0	0	0	0
≥19	0	0	0	0	0	0	0	0	0	0	0	1	0	0	0	0
≥20	0	0	0	0	0	0	0	0	0	0	0	1	0	0	0	0
≥21	0	0	0	0	0	0	0	0	0	0	0	1	0	0	0	0
≥22	0	0	0	0	0	0	0	0	0	0	0	1	0	0	0	0
≥23	0	0	0	0	0	0	0	0	0	0	0	1	0	0	0	0
≥24	0	0	0	0	0	0	0	0	0	0	0	1	0	0	0	0

TABLE 2-12

TOTAL NUMBER OF OCCURRENCES OF THE COMBINED PERSISTENCE OF WIND DIRECTION AND WIND SPEED ABOVE 8.2 METERS PER SECOND AT THE GREATER PITTSBURGH AIRPORT FOR THE PERIOD 1963 - 1964

Number of Hours of Persistence	Wind Direction (Sector)															
	N	NNE	NE	ENE	E	ESE	SE	SSE	S	SSW	SW	WSW	W	WNW	NW	NNW
≥1	7	1	1	8	1	2	4	2	3	9	80	217	182	126	70	27
≥2	0	0	0	2	0	0	0	1	0	0	14	63	53	30	15	6
≥3	0	0	0	0	0	0	0	0	0	0	4	34	21	14	3	2
≥4	0	0	0	0	0	0	0	0	0	0	2	12	9	4	2	2
≥5	0	0	0	0	0	0	0	0	0	0	1	8	8	2	0	1
≥6	0	0	0	0	0	0	0	0	0	0	0	6	4	2	0	0
≥7	0	0	0	0	0	0	0	0	0	0	0	5	2	2	0	0
≥8	0	0	0	0	0	0	0	0	0	0	0	2	0	1	0	0
≥9	0	0	0	0	0	0	0	0	0	0	0	2	0	1	0	0
≥10	0	0	0	0	0	0	0	0	0	0	0	2	0	0	0	0
≥11	0	0	0	0	0	0	0	0	0	0	0	1	0	0	0	0
≥12	0	0	0	0	0	0	0	0	0	0	0	1	0	0	0	0
≥13	0	0	0	0	0	0	0	0	0	0	0	1	0	0	0	0
≥14	0	0	0	0	0	0	0	0	0	0	0	1	0	0	0	0
≥15	0	0	0	0	0	0	0	0	0	0	0	1	0	0	0	0
≥16	0	0	0	0	0	0	0	0	0	0	0	0	0	0	0	0
≥17	0	0	0	0	0	0	0	0	0	0	0	0	0	0	0	0
≥18	0	0	0	0	0	0	0	0	0	0	0	0	0	0	0	0
≥19	0	0	0	0	0	0	0	0	0	0	0	0	0	0	0	0
≥20	0	0	0	0	0	0	0	0	0	0	0	0	0	0	0	0
≥21	0	0	0	0	0	0	0	0	0	0	0	0	0	0	0	0
≥22	0	0	0	0	0	0	0	0	0	0	0	0	0	0	0	0
≥23	0	0	0	0	0	0	0	0	0	0	0	0	0	0	0	0
≥24	0	0	0	0	0	0	0	0	0	0	0	0	0	0	0	0

pressure systems that have characteristic dimensions of at least several hundred kilometers. The Greater Pittsburgh Airport is approximately 85 kilometers northeast of the Mitchell and Kammer Power Plants.

SECTION 3

CALCULATION PROCEDURES AND RESULTS

3.1 MAXIMUM 3-HOUR AND 24-HOUR GROUND-LEVEL SO_2 CONCENTRATIONS PRODUCED BY EMISSIONS FROM THE MITCHELL AND KAMMER POWER PLANTS

When buoyant stack plumes are brought into contact with elevated terrain by turbulent mixing, the short-term concentrations at or near the terrain interface increase both with increasing wind speed and increasing terrain elevation. This differs from the flat terrain case where the maximum short-term ground-level concentrations produced by buoyant stack emissions occur when the wind speed reaches a critical value (the critical wind speed) determined by the stack parameters. Prior to calculating maximum 3-hour and 24-hour SO_2 ground-level concentrations, it is helpful to consider wind-persistence statistics, if available, in selecting an appropriate wind speed and the wind direction(s) for which this wind speed is most likely to persist for 3- and 24-hours. As mentioned in Section 2.2, wind-persistence statistics for the Greater Pittsburgh Airport were used to select the wind speed and wind directions for the Kammer and Mitchell short-term concentration calculations. Although the Greater Pittsburgh Airport wind-persistence statistics probably do not strictly apply to the area surrounding the Mittchell and Kammer Power Plants, the Greater Pittsburgh Airport is the closest station for which such data are available. The Greater Pittsburgh Airport data indicate that surface wind speeds from 5.1 to 8.2 meters per second can be expected to persist for 24 hours in combination with west winds about once per year and in combination with west-southwest winds about once every two years (see Table 2-10).

The short-term concentration model described in Section A.3 of Appendix A, including the adjustments for variations in terrain height described in Section A.5, was used with the stack and emissions data in Table 2-1 to calculate centerline profiles of 10-minute, 3-hour and 24-hour ground-level SO_2 concentrations produced by the

Kammer and Mitchell plumes for persistent west and west-southwest wind directions. The mean wind speed at a height of 373 meters above sea level (measurement height at the Greater Pittsburgh Airport) was set equal to 6.65 meters per second (the mean wind speed in the 5.1- to 8.2-meter per second category). Other meteorological inputs used in the short-term concentration calculations correspond to the parameter values for the Pasquill D stability category given in Tables 2-5 through 2-9 of Section 2. By definition, the Pasquill D stability category is the only stability category that can persist for 24 hours. As mentioned in Section 2.2, the lateral and vertical turbulent intensities were assumed to be equivalent for a 10-minute averaging time, and the $t^{1/5}$ law (Osipov, 1972) was used to extend the 10-minute lateral turbulent intensity to longer averaging times.

Figures 3-1 and 3-2 present the calculated profiles of centerline 3-hour and 24-hour ground-level SO_2 concentrations produced by the Mitchell and Kammer Power Plants, respectively. To aid in interpreting terrain effects, profiles of terrain elevation for distances of 1 to 21 kilometers downwind from each plant are shown at the bottom of the figures with the terrain heights in meters above sea level given at the right of each figure. In the Kammer calculations, the contribution of each stack to the ground-level concentration was calculated independently and the two contributions summed to yield the plotted values. Table 3-1 lists the calculated maximum 10-minute, 3-hour and 24-hour ground-level SO_2 concentrations for each of the centerline profiles plotted in the figures.

When the plumes from the Kammer and Mitchell Power Plants follow the Ohio River Valley rather than passing over the elevated terrain, the effective heights of the plumes above the ground are increased and the ground-level concentrations are decreased. Assuming the same meteorological inputs as in the previous calculations, Figure 3-3 shows the calculated profiles of centerline 3-hour and 24-hour ground-level SO_2 concentration on level terrain (terrain at the same elevations as the bases of the

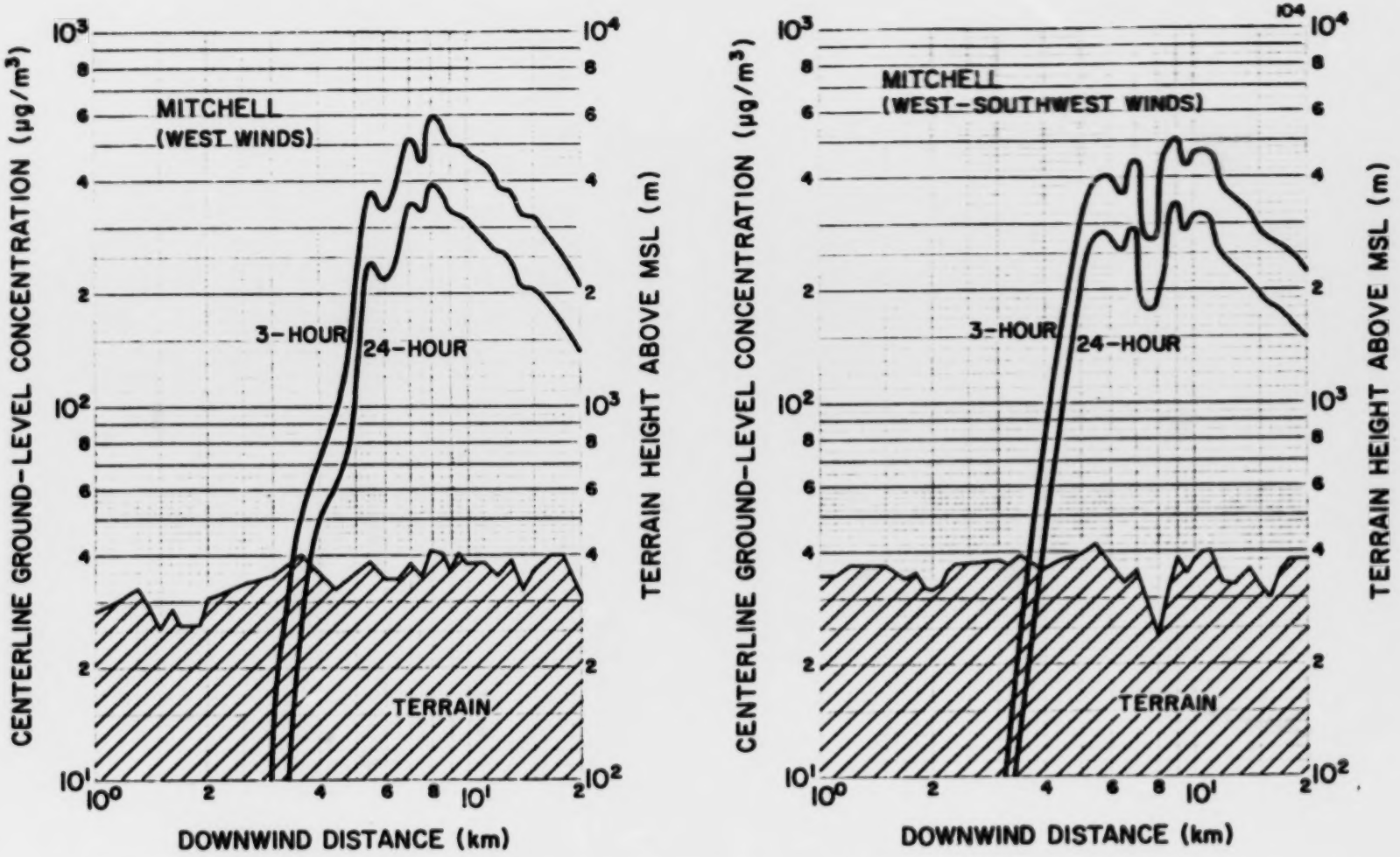

FIGURE 3-1. Calculated centerline profiles of maximum 3-hour and 24-hour ground-level SO_2 concentration in micrograms per cubic meter produced by the Mitchell plume with persistent west and west-southwest winds. Terrain heights are labeled at the right of the figures.

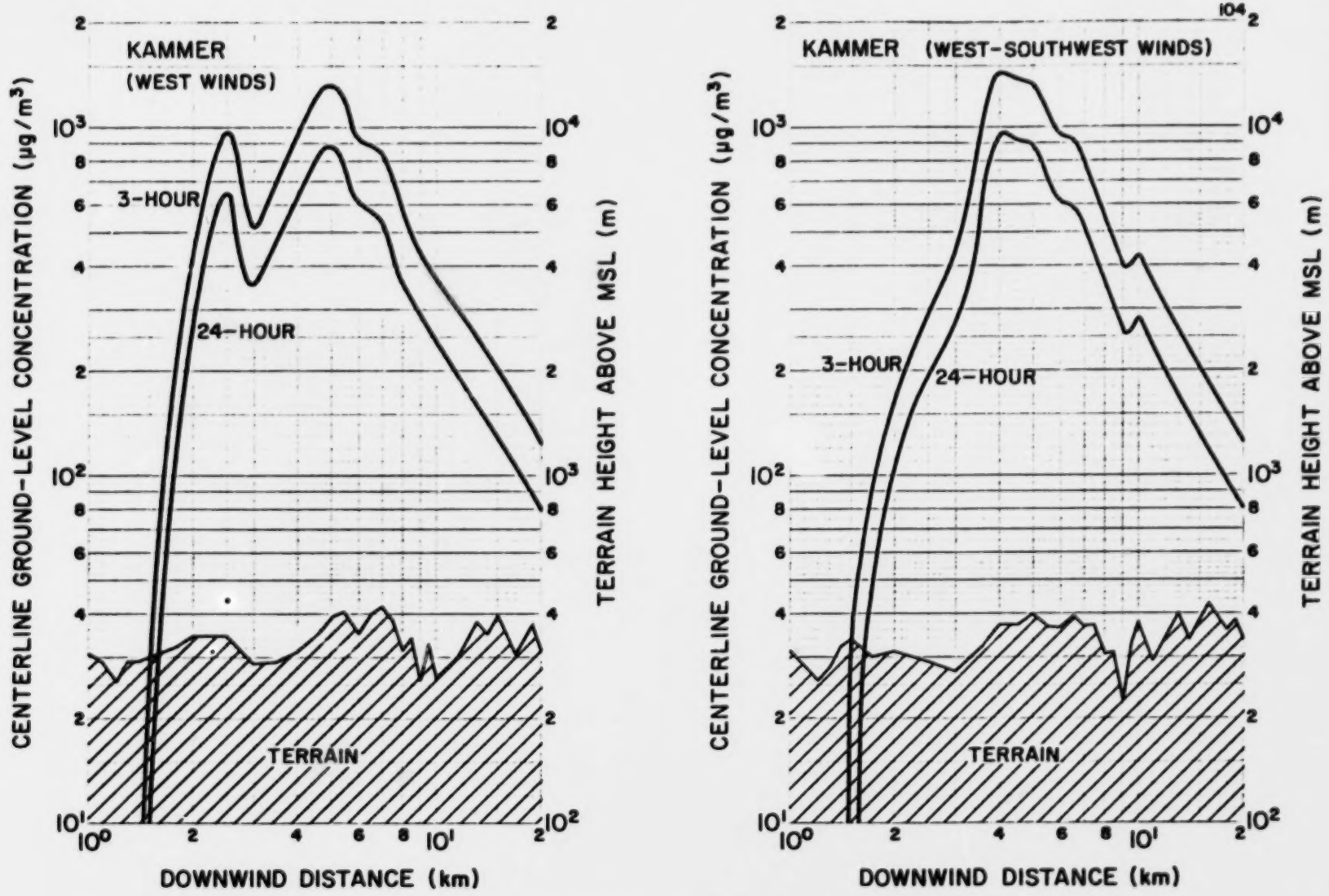

FIGURE 3-2. Calculated centerline profiles of maximum 3-hour and 24-hour ground-level SO_2 concentration in micrograms per cubic meter produced by the combined Kammer plumes with persistent west and west-southwest winds. Terrain heights are labeled at the right of the figures.

TABLE 3-1

CALCULATED MAXIMUM SHORT-TERM GROUND-LEVEL SO_2 CONCENTRATIONS WITH WEST AND WEST-SOUTHWEST WINDS*

Averaging Time	Concentration ($\mu g/m^3$)			
	Mitchell		Kammer	
	W Winds	WSW Winds	W Winds	WSW Winds
10 Minutes	1069	920	2405	2581
3 Hours	599	515	1347	1445
24 Hours	396	340	890	955

*Calculated concentrations do not include SO_2 background.

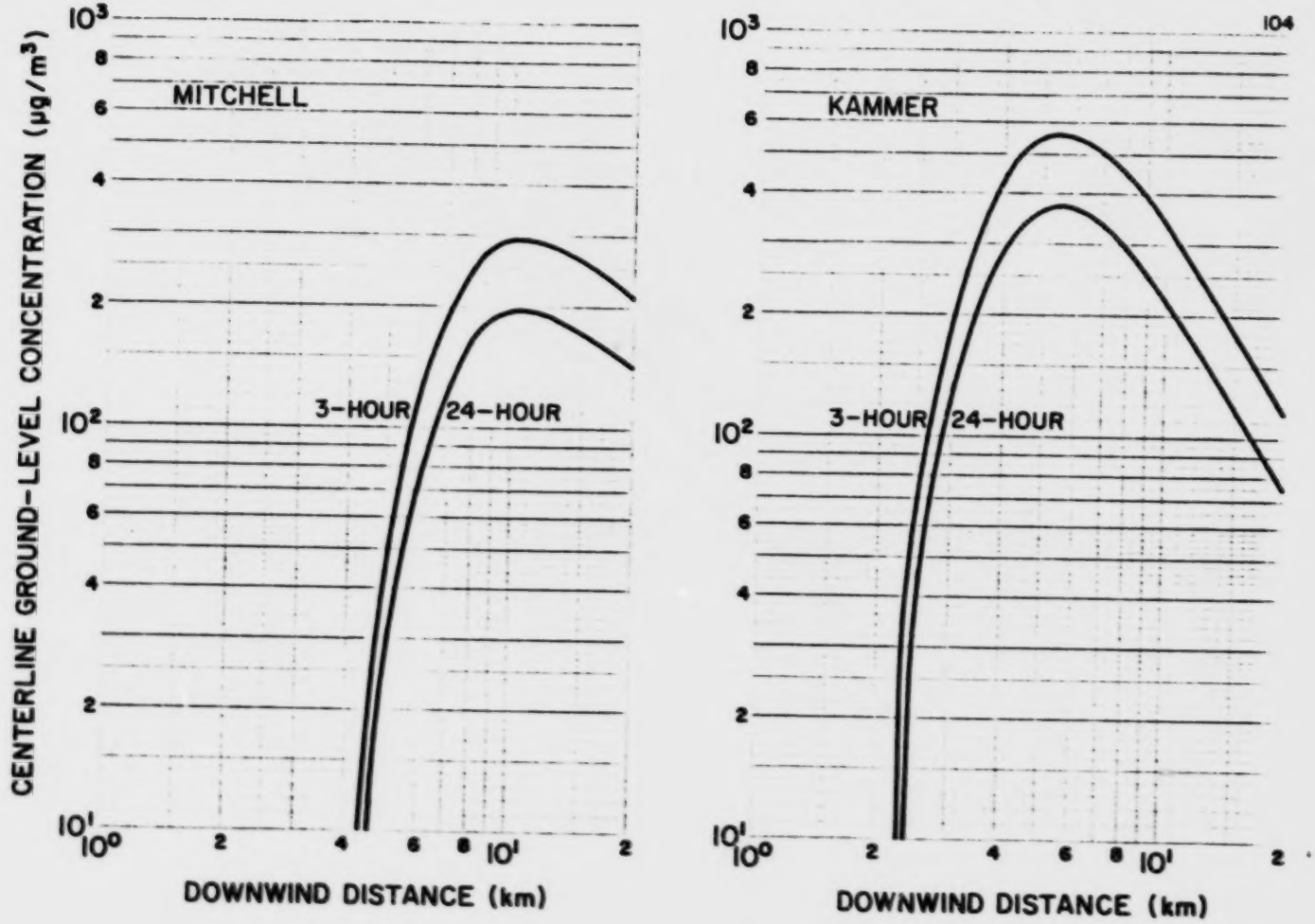

FIGURE 3-3. Calculated centerline profiles of maximum 3-hour and 24-hour ground-level SO_2 concentration in micrograms per cubic meter on terrain at the same elevation as the base of the stacks of the Mitchell and Kammer Power Plants.

stacks) for the Mitchell and Kammer Power Plants. The calculated maximum 10-minute, 3-hour and 24-hour ground-level concentrations on level terrain are listed in Table 3-2. Comparison of Tables 3-1 and 3-2 shows that terrain effects increase all the calculated short-term maximums for the Mitchell Power Plant by a factor of 2.0 for west winds and a factor of 1.74 for west-southwest winds. Similarly, terrain effects increase the calculated maximum short-term concentrations for the Kammer Power Plant by factors of 2.39 and 2.56 for west and west-southwest winds, respectively. The calculated maximum short-term concentrations for the Mitchell Power Plant occur at downwind distances of 8 to 9 kilometers on elevated terrain (see Figure 3-1) and 10 kilometers on level terrain (see Figure 3-3). The calculated maximum short-term concentrations for the Kammer Power Plant occur at downwind distances of 4 to 5.5 kilometers (see Figures 3-2 and 3-3). As noted previously, wind persistence statistics are lacking for the area in the vicinity of the Mitchell and Kammer plants. However, the terrain elevations on either side of the Ohio River Valley are typically 350 to 400 meters above mean sea level. The locations of areas of high terrain most likely to be affected by emissions from the Mitchell Power Plant are shown in Figure 3-4. The shaded areas in Figure 3-4 show elevations greater than 400 meters above mean sea level and the hatched areas show elevations greater than 335 meters above mean sea level. The locations of areas of high terrain most likely to be affected by emissions from the Kammer stacks are shown in Figure 3-5 where the elevations of the shaded and hatched areas are the same as in Figure 3-4.

3.2 EFFECTS OF THE INTERACTION OF THE KAMMER, MITCHELL AND BURGER PLUMES ON SHORT-TERM MAXIMUM GROUND-LEVEL CONCENTRATIONS

The maximum superposition of plumes from all three power plants occurs with south-southwest winds that align the plumes from the Mitchell and Burger Power Plants; the axes of the Kammer plumes are parallel to and about 1200 meters east of the axes of the Mitchell and Burger plumes. Figure 3-6 illustrates the approximate

TABLE 3-2

CALCULATED MAXIMUM SHORT-TERM GROUND-LEVEL SO_2 CONCENTRATIONS ON LEVEL TERRAIN*

Averaging Time	Concentration (μ g/m^3)	
	Mitchell	Kammer
10 Minutes	528	1006
3 Hours	296	563
24 Hours	195	372

*Calculated concentrations do not include SO_2 background.

FIGURE 3-4. Topographic map showing, within the concentric circles, the areas where high short-term ground-level SO_2 concentrations resulting from the Mitchell Power Plant emissions are most likely. The shaded areas represent terrain elevations of 400 meters (1300 feet) or more above sea level while the hatched areas represent terrain elevations between 335 meters (1100 feet) and 400 meters above sea level.

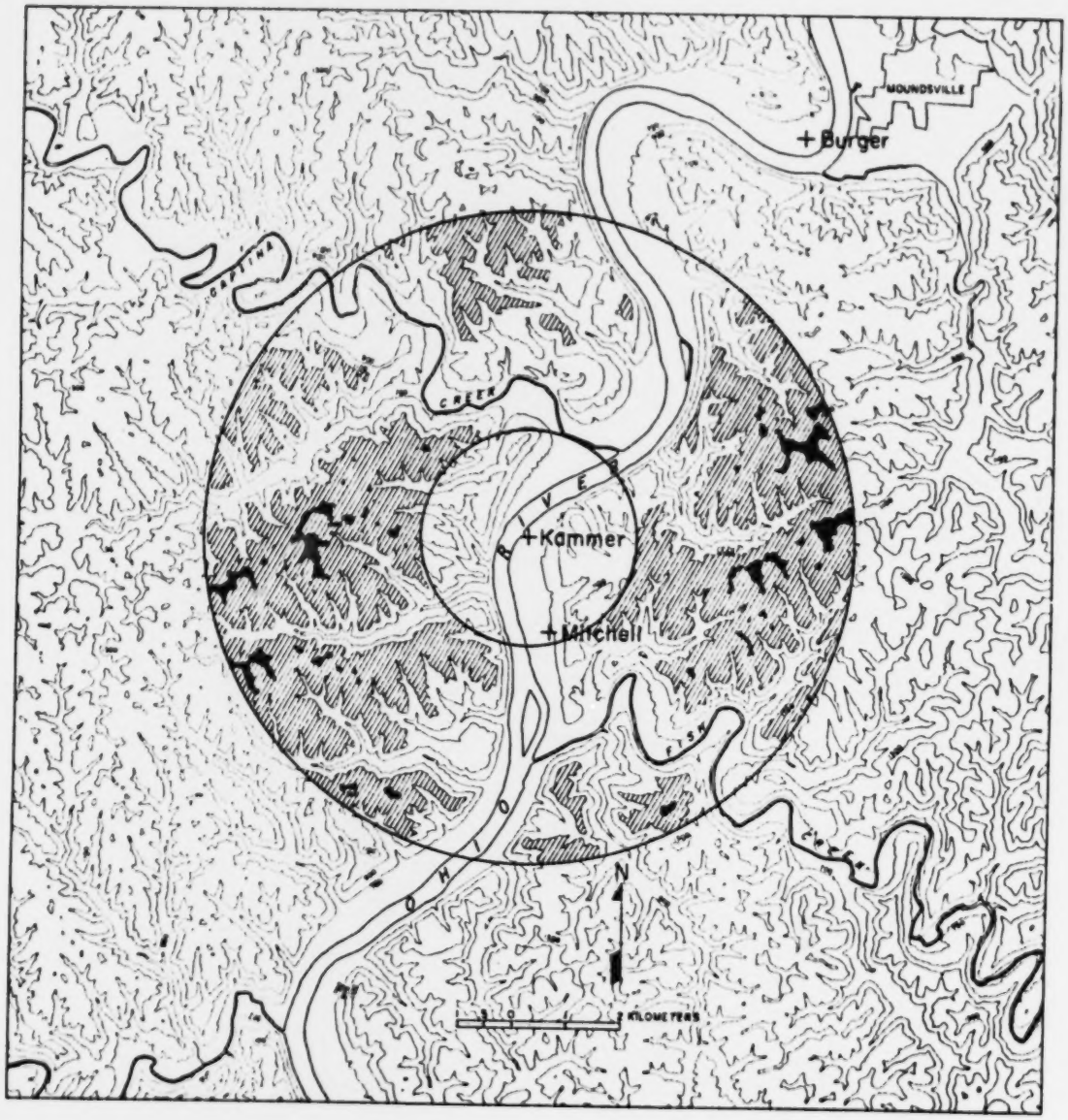

FIGURE 3-5. Topographic map showing, within the concentric circles, where high ground-level SO_2 concentrations resulting from the Kammer Power Plant emissions are most likely. The shaded areas represent terrain elevations of 400 meters (1300 feet) or more above sea level while the hatched areas represent terrain elevations between 335 meters (1100 feet) and 400 meters above sea level.

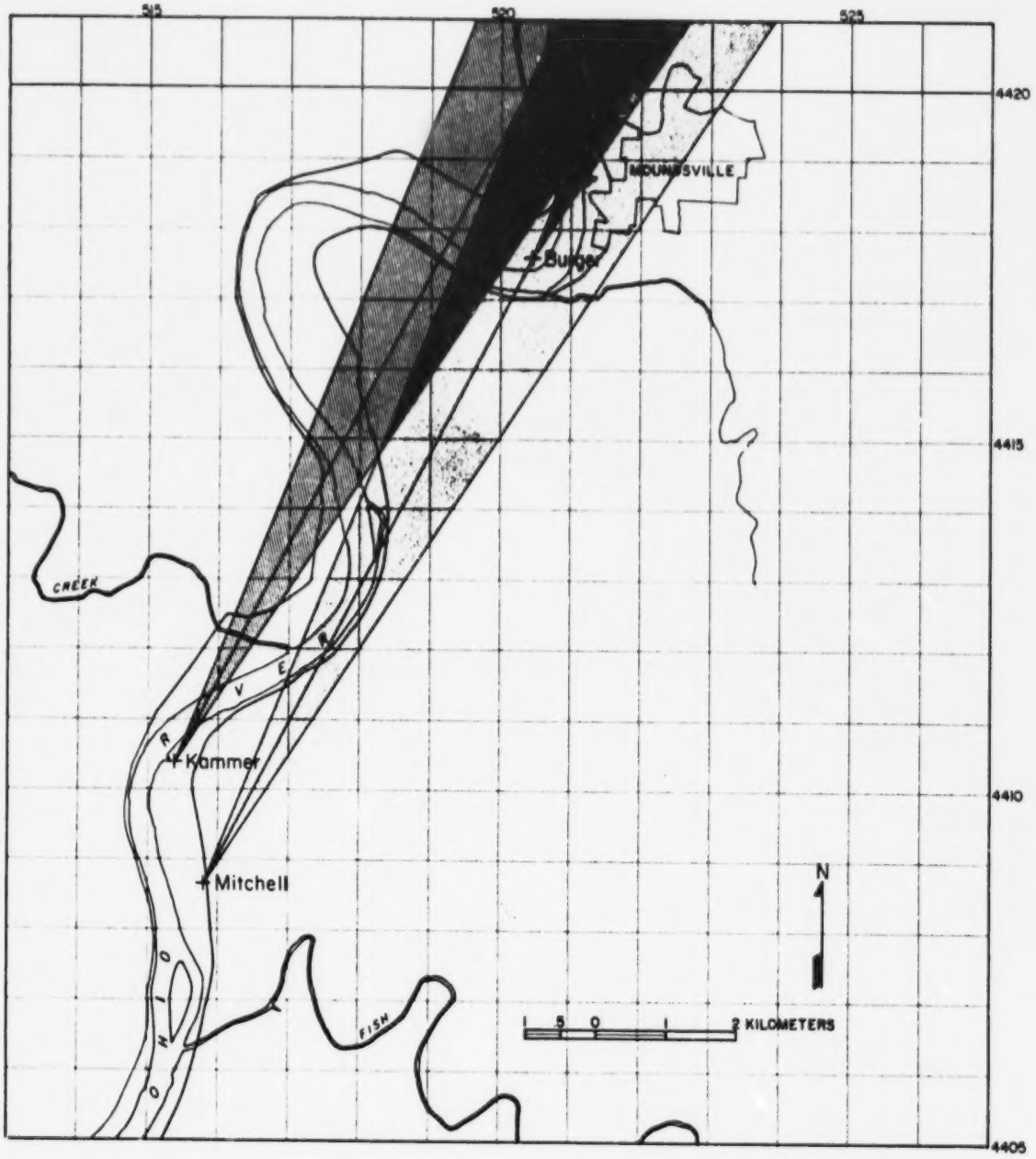

FIGURE 3-6. Approximate 24-hour plume boundaries (± 2.15 σ_y) for south-southwest winds and the Pasquill D stability category.

24-hour plume boundaries ($\pm 2.15\ \sigma_y$) for the Pasquill D stability category and south-southwest winds. With south-southwest winds and the same meteorological conditions assumed in the previous short-term concentration calculations, the calculated maximum ground-level SO_2 concentration produced by emissions from the Burger Power Plant occurs 4 kilometers north-northeast of the plant. This point is about 4.5 kilometers beyond the point of the maximum ground-level concentration produced by Mitchell emissions. Assuming 3- and 24-hour wind persistences, Table 3-3 lists the calculated maximum 3-hour and 24-hour ground-level SO_2 concentrations produced at this point by emissions from the three power plants.

The maximum superposition of the Mitchell and Kammer plumes occurs with south-southeast winds. Figure 3-7 shows the approximate 24-hour plume boundaries for the Pasquill D stability category with winds from the south-southeast. As indicated by the figure, the Burger plume does not affect the ambient air quality in the areas affected by emissions from the Mitchell and Kammer plants during periods of south-southeast winds. For south-southeast winds and the same meteorological conditions used in the preceding calculations, the maximum ground-level SO_2 concentration produced by Mitchell emissions is located 7.5 kilometers north-northwest of the Mitchell stack and the maximum ground-level concentration produced by Kammer emissions is located 6.5 kilometers north-northwest of the Mitchell stack. For the combined sources, the calculated maximum ground-level SO_2 concentration is located 6.5 kilometers north-northwest of the Mitchell stack (4.8 kilometers north-northwest of the Kammer plant). Assuming 3- and 24-hour wind persistences, Table 3-4 lists the calculated maximum 3-hour and 24-hour ground-level SO_2 concentrations produced by emissions from the Mitchell and Kammer plants.

There will also be some overlapping of the Mitchell and Kammer plumes during periods of persistent west and west-southwest winds that will increase the calculated maximum 3-hour and 24-hour ground-level SO_2 concentrations shown in Table 3-1 which were calculated separately for each plant. Table 3-5

TABLE 3-3

CALCULATED MAXIMUM SHORT-TERM GROUND-LEVEL SO_2 CONCENTRATIONS PRODUCED BY EMISSIONS FROM THE COMBINED SOURCES WITH SOUTH-SOUTHWEST WINDS*

Source	Concentration ($\mu g/m^3$)	
	3-Hour	24-Hour
Mitchell	264	174
Kammer	126	120
Burger	472	312
Combined Sources	862	606

*Calculated concentrations do not include SO_2 background

TABLE 3-4

CALCULATED MAXIMUM SHORT-TERM GROUND-LEVEL SO_2 CONCENTRATIONS PRODUCED BY EMISSIONS FROM THE COMBINED SOURCES WITH SOUTH-SOUTHEAST WINDS*

Source	Concentration ($\mu g/m^3$)	
	3-Hour	24-Hour
Mitchell	477	315
Kammer	1369	904
Combined Sources	1846	1219

* Calculated concentrations do not include SO_2 background

FIGURE 3-7. Approximate 24-hour plume boundaries ($\pm$ 2.15 σ_y) for south-south-east winds and the Pasquill D stability category.

shows the calculated maximum 3-hour and 24-hour ground-level SO_2 concentrations produced by the combined Kammer and Mitchell plumes for the west and west-southwest wind directions. Because the stabilization height of the Mitchell plume is much greater than the stabilization height of the Kammer plumes, the Mitchell plume comes in contact with the ground surface well beyond the downwind distances of the maximum ground-level concentrations produced by the Kammer plumes. The short-term maximum ground-level concentrations resulting from the combined Kammer and Mitchell plumes thus occur at the points of the Mitchell maximum ground-level concentrations. The entries in Table 3-5 show that the contributions of the Kammer plumes increase as the averaging time increases from 3 to 24 hours. This is explained by the increase in the Kammer plume widths with averaging time which in effect brings the Mitchell plume centerline closer in terms of the σ_y of the combined Kammer plumes to the centerline of the combined Kammer plumes. This more than offsets the decrease in the centerline concentration of the combined Kammer plumes caused by the increase in σ_y with averaging time. With winds from the west or west-southwest, the Burger plume does not interact with the Kammer and Mitchell plumes at downwind distances where the Burger emissions can contribute significantly to the combined maximum ground-level concentrations.

Comparison of Tables 3-3, 3-4 and 3-5 shows that persistent south-southeast winds lead to the highest calculated short-term concentrations for the combined sources. As shown in Table 3-4, only the Mitchell and Kammer plumes are superposed with Kammer contributing 70 to 75 percent of the total. The second highest calculated short-term concentrations for the combined sources occur with persistent south-southwest winds. In this case, the plumes from all three power plants are superposed with Burger contributing approximately 50 percent of the total.

3.3 ANNUAL AVERAGE SO_2 CONCENTRATIONS PRODUCED BY EMISSIONS FROM THE MITTCHELL AND KAMMER POWER PLANTS

The stack and emissions data in Table 2-1 and the annual meteorological inputs in Section 2.2 and Appendix B were used with the long-term concentration

TABLE 3-5

CALCULATED MAXIMUM 3-HOUR AND 24-HOUR SO_2 CONCENTRATIONS PRODUCED BY THE EMISSIONS FROM THE COMBINED SOURCES WITH WEST AND WEST-SOUTHWEST WINDS*

Source	Concentration (μ g/m^3)	
	3-Hour	24-Hour
(a) West Winds		
Mitchell	599	396
Kammer	37	118
Combined Sources	636	514
(b) West-Southwest Winds		
Mitchell	515	340
Kammer	34	108
Combined Sources	549	448

*Calculated concentrations do not include SO_2 background.

model described in Section A. 4 of Appendix A to calculate average annual ground-level SO_2 concentration patterns for the Kammer and Mitchell Power Plants. Concentrations were calculated at 651 grid points, spaced at regular intervals of 1 kilometer, on a 30-kilometer by 20-kilometer grid. Terrain elevations for all the grid points were obtained from topographic maps of the area and were included in the calculations following the procedures outlined in Section A. 5 of Appendix A.

Figures 3-8 and 3-9 show the calculated isopleths of annual average ground-level SO_2 concentration in micrograms per cubic meter produced by emissions from the Mitchell and Kammer plants, respectively. The annual concentration isopleths for the combined sources are shown in Figure 3-10. The Universal Transverse Mercator (UTM) X and Y coordinates for the calculation grid are entered along the bottom and at the right of each figure. As shown by Figure 3-8, SO_2 emissions from the Mitchell Power Plant alone result in maximum annual average ground-level concentrations of 30 micrograms per cubic meter over an area of 4 square kilometers centered approximately 8 kilometers east-southeast of the Mitchell Power Plant. Figure 3-9 shows that emissions from the Kammer Power Plant alone result in maximum annual average concentrations of 80 to 100 micrograms per cubic meter over an area of 5 or 6 square kilometers centered about 3. 5 kilometers east-southeast of the Kammer Power Plant. Figure 3-10 shows that the combined emissions from the Mitchell and Kammer stacks result in maximum annual average concentrations of 80 to 100 micrograms per cubic meter over an area of about 14 square kilometers centered about 4 kilometers east of the Kammer Power Plant. The location and magnitude of the calculated maximum annual average ground-level SO_2 concentration for each source and for the combined sources are listed in Table 3-6.

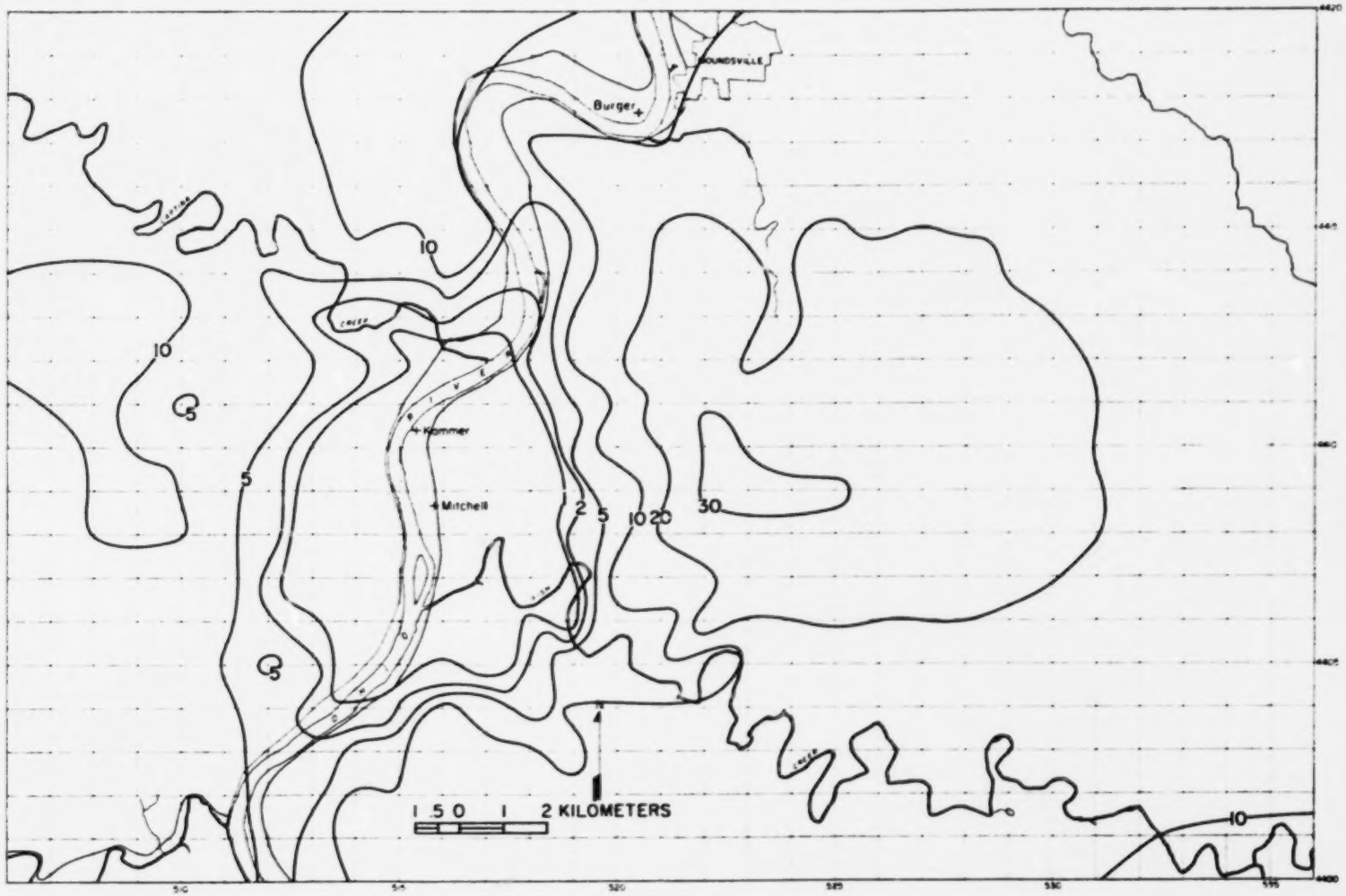

FIGURE 3-8. Calculated isopleths of annual average ground-level SO_2 concentration in micrograms per cubic meter produced by emissions from the Mitchell Power Plant.

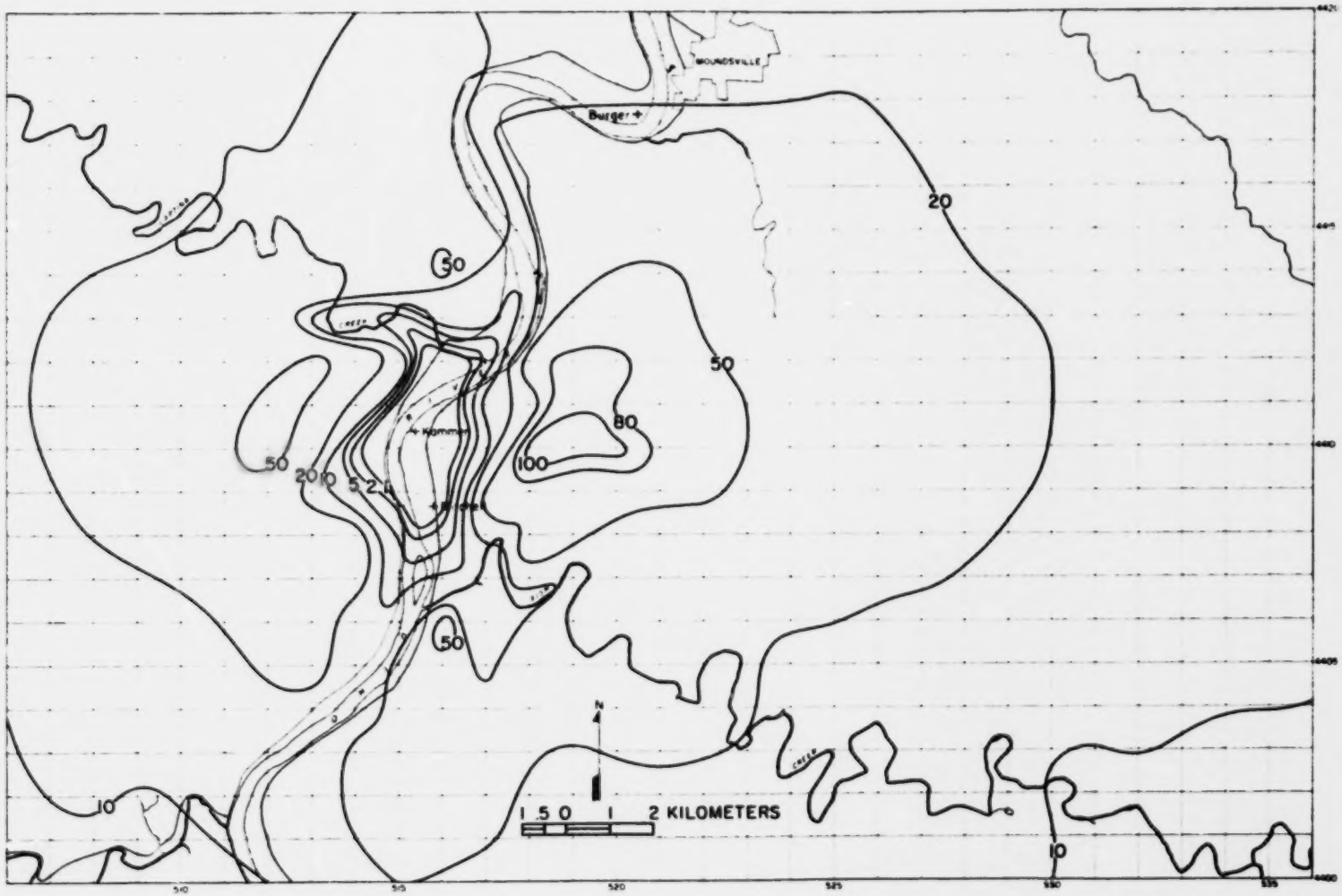

FIGURE 3-9. Calculated isopleths of annual average ground-level SO_2 concentration in micrograms per cubic meter produced by emissions from the Kammer Power Plant.

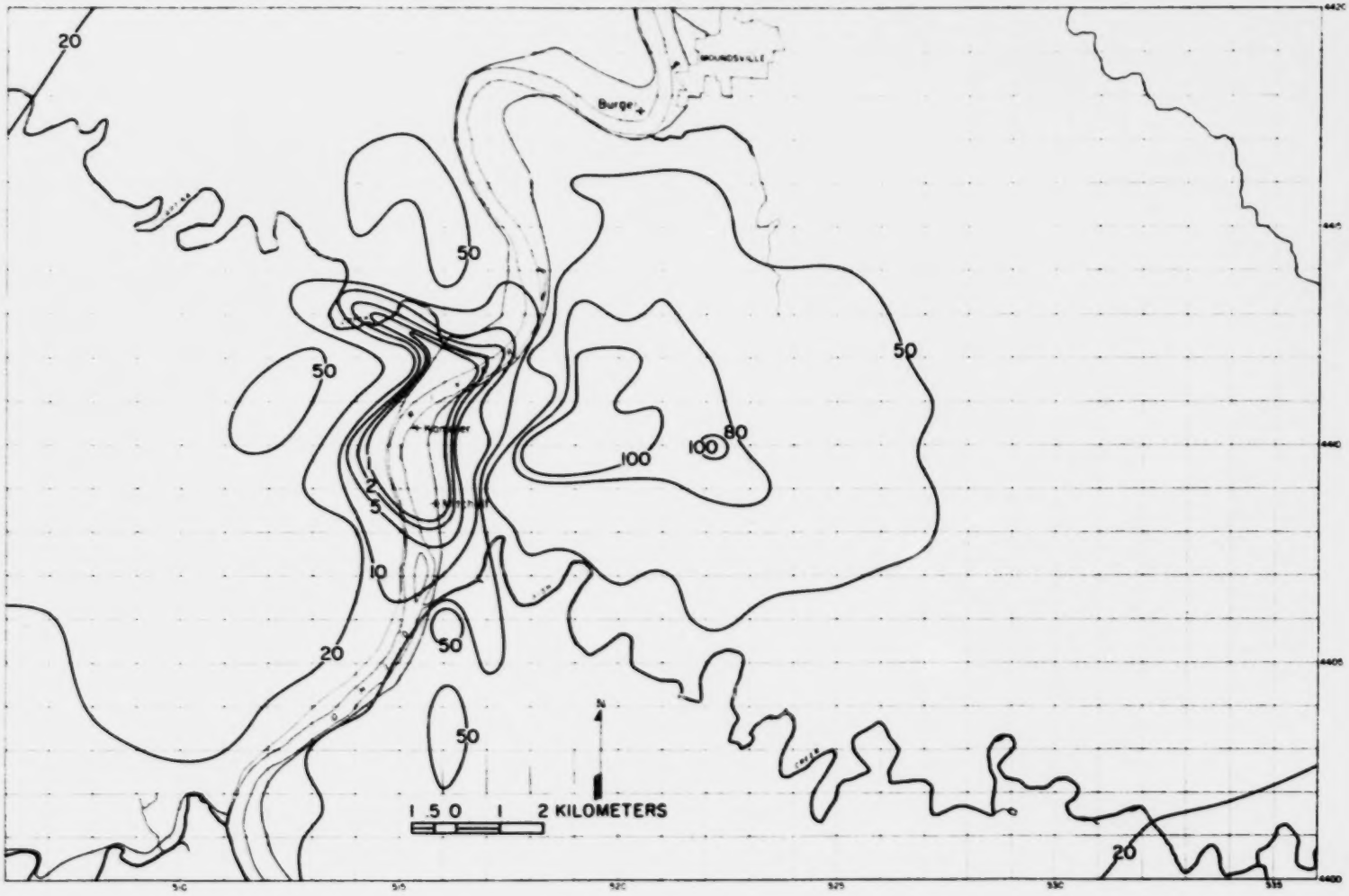

FIGURE 3-10. Calculated isopleths of annual average ground-level SO_2 concentration in micrograms per cubic meter produced by the combined emissions from the Mitchell and Kammer Power Plants.

TABLE 3-6

LOCATIONS AND MAGNITUDES OF CALCULATED
MAXIMUM ANNUAL AVERAGE GROUND-LEVEL SO_2 CONCENTRATION *

Source	Maximum Concentration ($\mu g/m^3$)	Location	
		UTM X (km)	UTM Y (km)
Mitchell	38.2	522	4410
Kammer	129.7	519	4410
Combined Sources	134.8	519	4410

* Calculated concentrations do not include So_2 background

SECTION 4
SUMMARY OF RESULTS

4.1 CALCULATED MAXIMUM SHORT-TERM CONCENTRATIONS

Table 4-1 lists, for the Mitchell and Kammer Plants individually, the maximum 3-hour and 24-hour ground-level SO_2 concentrations calculated for five wind directions. The calculated 3-hour and 24-hour concentrations in Table 4-1 assume that moderate to strong winds persist from the indicated wind directions for 3 and 24 hours, respectively. The calculated concentrations do not include any SO_2 background or the contribution, if any, of the other sources in the area. The locations of the calculated maximum concentrations are shown by the numbered filled circles and squares in Figure 4-1; the circles show the locations of maximum concentrations produced by Kammer emissions and the squares show the locations of maximum concentrations produced by Mitchell emissions. Point Number 1 for Mitchell is not shown in Figure 4-1 because it is located approximately 1 kilometer below the southern boundary of the figure.

Inspection of Table 4-1 and Figure 4-1 shows that winds from the north-northeast or south-southwest result in calculated maximum ground-level SO_2 concentrations for both the Kammer and Mitchell Power Plants that are located in the Ohio River Valley. With winds from the west, west-southwest and south-southeast, the calculated maximum ground-level concentrations for both plants are located on elevated terrain. For the Kammer Power Plant, the calculated maximum concentrations on elevated terrain differ by less than 10 percent and are all approximately 2 to 3 times larger than the corresponding concentrations calculated for points in the Ohio River Valley. Similarly, the calculated maximum concentrations for the Mitchell Power Plant that occur on elevated terrain differ by about 10 percent and are all approximately twice as large as the corresponding concentrations calculated for points in the valley.

TABLE 4-1

SUMMARY OF CALCULATED MAXIMUM 3-HOUR AND 24-HOUR GROUND-LEVEL SO_2 CONCENTRATIONS PRODUCED BY KAMMER AND MITCHELL SEPARATELY*

Wind Direction	Concentration ($\mu g/m^3$)		Distance (km)	Bearing (deg)
	3-Hour	24-Hour		
(a) Kammer				
(1) North- Northeast**	563	372	5.5	190
(2) South-Southwest**	563	372	5.5	015
(3) West	1347	890	5.0	090
(4) West-Southwest	1445	955	4.0	068
(5) South-Southeast	1369	904	4.8	346
(b) Mitchell				
(1) North-Northeast**	296	195	10.0	190
(2) South-Southwest**	296	195	10.0	015
(3) West	599	396	8.0	090
(4) West-Southwest	515	340	9.0	068
(5) South-Southeast	526	347	7.5	346

* Calculated concentrations do not include SO_2 background.

** Maximums occur on terrain with same elevation as stack base.

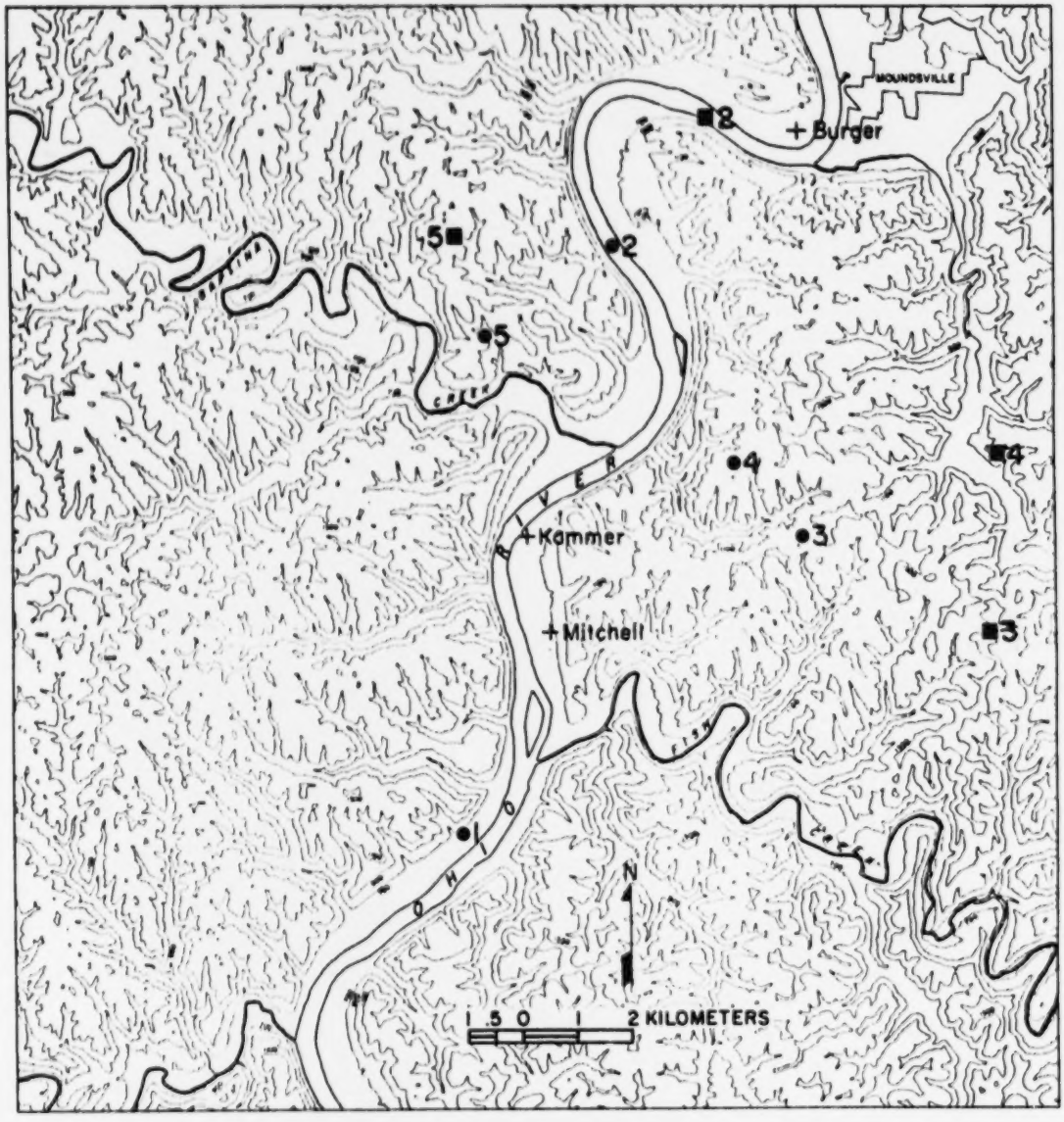

FIGURE 4-1. Topographic map of the area surrounding the Mitchell and Kammer Power Plants showing the locations of the calculated maximum ground-level SO_2 concentrations produced by emissions from the Kammer Power Plant (filled circles) and the Mitchell Power Plant (filled squares). The numbers refer to the cases in Table 4-1.

Table 4-2 lists the calculated maximum 3-hour and 24-hour ground-level SO_2 concentrations produced by the combined emissions from the Kammer, Mitchell and Burger Power Plants. The calculated 3-hour and 24-hour concentrations in Table 4-2 assume that moderate-to-strong winds persist from the indicated wind directions for 3 and 24 hours, respectively. The calculated concentrations do not include any SO_2 background. The locations of the calculated maximum concentrations are shown by the filled circles in Figure 4-2. Point Number 3 is not shown in Figure 4-2 because it is located about 1.5 kilometers beyond the northern boundary of the figure.

Table 4-2 shows that, for west and west-southwest winds, the Burger and Mitchell plumes do not contribute at the points of the maximum ground-level SO_2 concentrations calculated for the Kammer plumes, but the Kammer plumes contribute at the points of the maximum ground-level SO_2 concentrations calculated for the Mitchell plume. When the wind direction is south southwest, both the Mitchell and Kammer plumes interact with the Burger plume to produce calculated maximum 3-hour and 24-hour ground-level SO_2 concentrations approximately 4 kilometers north northeast of the Burger Power Plant (the point of the calculated maximum 3-hour and 24-hour concentrations for Burger). With south-southeast winds, the Mitchell and Kammer plumes are superimposed and the maximum 3-hour and 24-hour concentrations calculated for the combined sources occur at the point of the maximum 3-hour and 24-hour concentrations calculated for the Kammer plant. The Burger plume does not interact with the Mitchell and Kammer plumes during periods of south-southeast winds.

As noted above, the calculated concentrations listed in Tables 4-1 and 4-2 do not include any SO_2 background. To the best of our knowledge, the only onsite measurements of the SO_2 background are those obtained during the sampling program conducted by the EPA Environmental Monitoring and Support Laboratory (see Appendix C). EMSL found that the short-term background SO_2 concentration varied

TABLE 4-2

SUMMARY OF CALCULATED MAXIMUM 3-HOUR AND 24-HOUR GROUND-LEVEL SO_2 CONCENTRATIONS PRODUCED BY THE COMBINED EMISSIONS FOR THE KAMMER, MITCHELL AND BURGER POWER PLANTS*

Wind Direction	Source(s)	Concentration ($\mu g/m^3$)		Distance (km)**	Bearing (deg)**
		3-Hour	24-Hour		
(1) West	Mitchell	599	396		
	Kammer	37	118		
	Combined Sources	636	514	8.0	090
(2) West-Southwest	Mitchell	515	340		
	Kammer	34	108		
	Combined Sources	549	448	9.0	068
(3) South-Southwest	Mitchell	264	174		
	Kammer	126	120		
	Burger	472	312		
	Combined Sources	862	606	14.5	027
(4) South-Southeast	Mitchell	477	315		
	Kammer	1369	904		
	Combined Sources	1846	1219	7.5	346

* Calculated concentrations do not include SO_2 background

** From the Mitchell stack

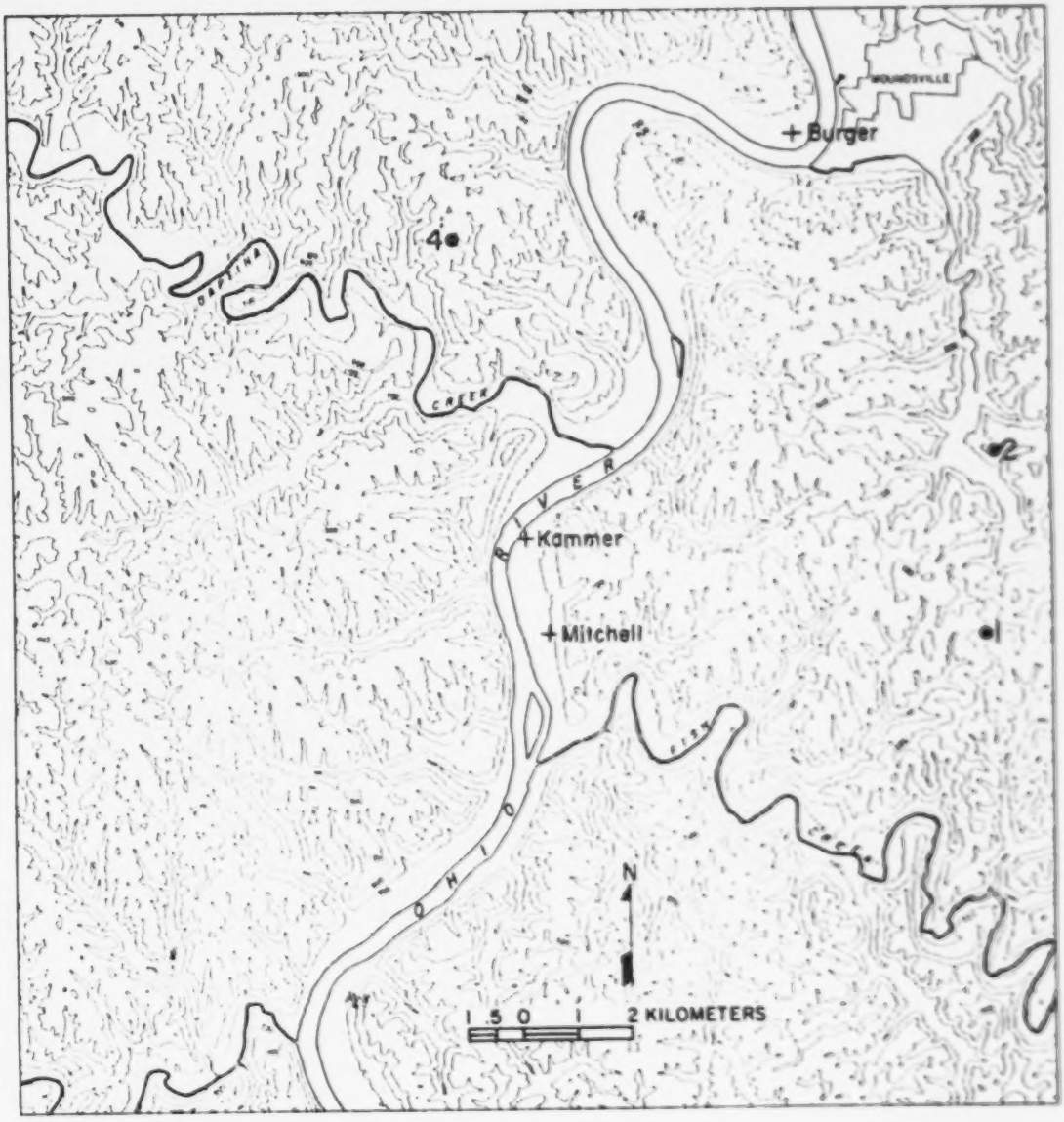

FIGURE 4-2. Topographic map of the area surrounding the Mitchell and Kammer Power Plants. The filled circles show the locations of the calculated maximum ground-level SO_2 concentrations produced by emissions from the combined sources. The numbers refer to the cases in Table 4-2.

from about 0.01 to 0.05 parts per million (25 to 130 micrograms per cubic meter). Background SO_2 measurements cited in a recent draft Ohio State Implementation Plan for SO_2 prepared by EPA show the second highest 24-hour background SO_2 concentrations observed over a 1-year period in three different Ohio counties were approximately 100 micrograms per cubic meter. In each county, the background estimate was based on SO_2 concentration measurements in the vicinity of an isolated point source during 24-hour periods when the monitor was upwind of the point source. We estimate that there are 24-hour periods when the background SO_2 concentration in the vicinity of the Mitchell and Kammer Power Plants is 50 to 100 micrograms per cubic meter and 3-hour periods when the background is 100 to 150 micrograms per cubic meter.

4.2 CALCULATED MAXIMUM ANNUAL CONCENTRATIONS

Table 4-3 lists the magnitudes and locations of the calculated maximum annual average ground-level SO_2 concentrations produced by emissions from the Mitchell Power Plant, the Kammer Power Plant and the combined emissions from the Mitchell and Kammer Power Plants. The calculated annual concentrations in Table 4-3 do not include any background SO_2. Although the Burger Power Plant was not included in the annual concentration calculations, the annual wind distribution for the Greater Pittsburgh Airport (see Appendix B) indicates that the contribution of Burger emissions to the annual concentrations in the area of maximum annual average concentrations produced by emissions from the Kammer and Mitchell Power Plants is small.

In the absence of long-term ambient air quality measurements in the vicinity of the Mitchell and Kammer Power Plants, we can only speculate about the value of the annual background SO_2 concentration. As noted above, EMSL found that the minimum short-term background concentration was about 0.01 parts per million (25 micrograms per cubic meter). Thus, the annual average SO_2 background is probably at least 25 micrograms per cubic meter.

TABLE 4-3

LOCATIONS AND MAGNITUDES OF CALCULATED
MAXIMUM ANNUAL AVERAGE GROUND-LEVEL SO_2 CONCENTRATION *

Source	Maximum Concentration ($\mu g/m^3$)	Location	
		UTM X (km)	UTM Y (km)
Mitchell	38.2	522	4410
Kammer	129.7	519	4410
Mitchell and Kammer	134.8	519	4410

* Calculated concentrations do not include So_2 background

4.3 IDENTIFICATION OF MAJOR AREAS OF UNCERTAINTY IN THE DIFFUSION-MODEL CALCULATIONS

In using the diffusion-model calculations presented in Section 3 and summarized in Sections 4.1 and 4.2 to assess the air quality impact of SO_2 emissions from the Kammer and Mitchell Power Plants, there are a number of factors affecting the accuracy of these calculations that must be recognized. The most important areas of uncertainty affecting the accuracy of the diffusion-model calculations and their use in assessing the impact of the power plant emissions on ambient air quality are:

- The representativeness of the emissions data and stack parameters in Tables 2-1 and 2-2
- The accuracy of the procedures used in the diffusion-model calculations to account for the effects of elevated terrain on ground-level SO_2 concentrations
- The representativeness of the meteorological inputs, including wind persistence, and the diffusion coefficients used in the model calculations

With respect to the representativeness of the source parameters and emissions data, our only basis for making any judgment is the emissions data obtained for the Kammer and Mitchell Power Plants for the period of the EPA Environmental Monitoring and Support Laboratory (EMSL) field measurement program (see Appendix C). For periods when the plants were operating at or near full load, the reported volumetric and SO_2 emission rates are very close to the values listed in Table 2-1. We have no basis for making any judgment about the representativeness of the source and emissions data for the Burger Power Plant, and we have assumed that the data supplied by the West Virginia Air Pollution

Control Commission and listed in Table 2-2 are applicable. Also, as discussed in Section 2.1, the Froude number of the Burger plant is in a range where exit-velocity (downwash) restrictions on buoyant plume rise may or may not occur. In the absence of direct measurements of the behavior of the Burger plume during periods when the wind speed equals or exceeds the stack exit velocity, we assumed that exit-velocity restrictions on plume rise occur. Thus, the maximum ground-level SO_2 concentrations calculated for the Burger plant may be safe-sided.

Our analysis of the EMSL SO_2 concentration measurements discussed in Appendix C indicates that the presence of elevated terrain can affect the ground-level concentrations produced by stack emissions. Two EMSL trials measured short-term ground-level SO_2 concentrations during periods when the Kammer plumes were observed to be impacting on nearby elevated terrain and the correspondence between the observed concentrations and the concentrations calculated using the terrain-adjustment procedures described in Section A.5 of Appendix A is good. If terrain effects are not included in the calculations, the calculated concentrations are substantially lower than the observed concentrations. The same terrain-adjustment procedures have been used in previous studies of SO_2 sources located in complex terrain (Cramer, et al., 1975; Cramer and Bowers, 1976; and Cramer, et al., 1976), and the correspondence between calculated and observed short-term and annual average ground-level SO_2 concentrations has generally been excellent. We therefore conclude that the procedures used in the diffusion-model calculations to account for the effects of elevated terrain on ground-level SO_2 concentrations are appropriate and yield concentration estimates that are in accord with observations.

The EMSL measurements also provided an opportunity to test the representativeness of the meteorological inputs and diffusion coefficients used in the model calculations. During our analysis of the EMSL data, we found that meteorological inputs to the diffusion models derived from surface and upper-air

meteorological data for the Greater Pittsburgh Airport are, at least on the average, very similar to the corresponding inputs derived from data for the Wheeling, West Virginia Airport and from onsite meteorological measurements made by EMSL. The correspondence between calculated and observed axial SO_2 concentrations for the Mitchell and Kammer plumes indicates that the diffusion coefficients used in the model calculations are applicable, although there is a possibility that the short-term model overestimates lateral plume growth at downwind distances on the order of 10 kilometers and thus underestimates ground-level concentrations.

In calculating the maximum 3-hour and 24-hour ground-level SO_2 concentrations in Tables 4-1 and 4-2, we assumed that moderate-to-strong winds persisted from the indicated wind directions for 3 and 24 hours, respectively. Wind-persistense statistics are lacking for the area in the vicinity of the Mitchell and Kammer Power Plants, and accurate estimates of the wind persistence at the plume stabilization heights (typically 400 meters above the surface for the Kammer plumes and 1000 meters above the surface for the Mitchell plume) are not possible. Wind-persistence statistics for the Greater Pittsburgh Airport indicate that moderate-to-strong west or west-southwest surface winds can be expected to persist for 24 or more hours once or twice per year. It is likely that a similar annual frequency of 24-hour wind persistence applies to the area surrounding the Mitchell and Kammer Power Plants. However, it is not possible to specify with certainty the wind-direction sectors associated with these persistent winds.

REFERENCES

Briggs, G. A., 1971: Some recent analyses of plume rise observations. In Proceedings of the Second International Clean Air Congress, Academic Press, New York.

Briggs, G. A., 1972: Chimney plumes in neutral and stable surroungings. Atm. Env., 6(7), 507-510.

Calder, K. L., 1971: A climatological model for multiple source urban air pollution. Proc. 2nd Meeting of the Expert Panel on Air Pollution Modeling, NATO Committee on the Challenges of Modern Society, Paris, France. July 1971, 33.

Cramer, H. E., et al., 1972: Development of dosage models and concepts. GCA Corporation Final Report under Contract DAAD09-67-C-0020(R) with the U. S. Army, Deseret Test Center Report DTC-TR-72-609, Fort Douglas, Utah.

Cramer, H. E., H. V. Geary and J. F. Bowers, 1975: Diffusion-model calculations of long-term and short-term ground-level SO_2 concentrations in Allegheny County, Pennsylvania. EPA 903/9-75-018, U. S. Environmental Protection Agency, Region III, Philadelphia, Pennsylvania.

Cramer, H. E. and J. F. Bowers, 1976: Calculated impact on ambient air quality of SO_2 emissions from the Mohave Power Plant (Draft). H. E. Cramer Company Technical Report TR 76-107-01 prepared for the U. S. Environmental Protection Agency, Region IX, San Francisco, California.

Cramer, H. E., J. F. Bowers and H. V. Geary, 1976: Assessment of the air quality impact of SO_2 emissions from the ASARCO-Tacoma smelter (Draft). H. E. Cramer Company Technical Report TR 76-105-01, prepared for the U. S. Environmental Protection Agency, Region X, Seattle, Washington.

DeMarrais, G. A., 1959: Wind speed profiles at Brookhaven National Laboratory. J. Met., 16, 181-190.

Environmental Data Service, 1966: Tabulation III, daily mixing depths and average wind speeds--Pittsburgh, Pennsylvania. Job No. 6234, National Climatic Center, Federal Building, Asheville, N. C.

Johnson, F. G., R. B. Evans and T. M. Zeller, 1976: Airborne measurements of power plant plumes in West Virginia, 1975. EPA Draft Report, Environmental Monitoring and Support Laboratory, U. S. Environmental Protection Agency, Las Vegas, Nevada.

Luna, R. E. and H. W. Church, 1971: A comparison of turbulence intensity and stability ratio measurements to Pasquill turbulence types. Paper presented at a Conference on Air Pollution Meteorology, Raleigh, N. C., April 5-9, 1971.

Osipov, Y. S., 1972: Diffusion from a point source of finite time of action. In AICE Survey of USSR Air Pollution Literature - Volume XII, distributed by National Technical Information Service, Springfield, Virginia.

Pasquill, F., 1961: The estimation of the dispersion of windborne material. Met. Mag., 90, 33-49.

Pasquill, F., 1962: Atmospheric Diffusion, D. Van Nostrand Co., Ltd., London, 297.

Turner, D. B., 1964: A diffusion model for an urban area. J. Appl. Meteor., 3 (1), 83-91.

APPENDIX A

MATHEMATICAL MODELS USED TO CALCULATE GROUND-LEVEL CONCENTRATIONS

A.1 INTRODUCTION

The computerized diffusion models described in this appendix fall into two general categories: (1) Short-term models for calculating time-averaged ground-level concentrations for averaging times of 1, 3, 8 and 24 hours; (2) Long-term models for calculating seasonal and annual ground-level concentrations. Both the short-term and long-term concentration models are modified versions of the Gaussian plume model for continuous sources described by Pasquill (1962). In the short-term model, the plume is assumed to have Gaussian vertical and lateral concentration distributions. The long-term model is a sector model similar in form to the Environmental Protection Agency's Climatological Dispersion Model (Calder, 1971) in which the vertical concentration distribution is assumed to be Gaussian and the lateral concentration distribution within a sector is rectangular (a smoothing function is used to eliminate sharp discontinuities at the sector boundaries). The σ_z vertical expansion curves and the σ_y lateral expansion curves are determined by using turbulent intensities in simple power-law expressions that include the effects of initial source dimensions. In both the short-term and long-term models, buoyant plume rise is calculated by means of the Briggs (1971) plume-rise formulas. An exponent law is used to adjust the surface wind speed to the source height for plume-rise calculations and to the plume stabilization height for concentration calculations. Both the short-term and the long-term models contain provisions to account for the effects of complex terrain.

Table A-1 lists the hourly meteorological inputs required by the short-term concentration model. Lateral and vertical turbulent intensities σ'_A and σ'_E

TABLE A-1

HOURLY METEOROLOGICAL INPUTS REQUIRED BY THE SHORT-TERM CONCENTRATION MODEL

Parameter	Definition
$\bar{u}_R$	Mean wind speed at height z_R
θ	Mean wind direction at height z_R
p	Wind-profile exponent
σ'_A	Wind azimuth-angle standard deviation in radians
σ'_E	Wind elevation-angle standard deviation in radians
T_a	Ambient air temperature (^oK)
H_m	Depth of surface mixing layer
$\frac{\partial\theta}{\partial z}$	Vertical potential temperature gradient

may be directly specified or may be assigned on the basis of the Pasquill stability category. The Pasquill stability category is determined from surface weather observations using the Turner (1964) wind-speed and solar-index values. Mixing depths may be obtained from rawinsonde or pibal measurements, or they may be assigned on the basis of tabulations of the frequency of occurrence of wind speed and mixing depth (available from the National Climatic Center for synoptic rawinsonde stations). Potential temperature gradients may be measured or assigned on the basis of climatology.

Table A-2 lists the meteorological inputs required by the long-term concentration model. Joint-frequency distributions of wind-speed and wind-direction categories according to the Pasquill stability categories may be obtained from the National Climatic Center. Alternately, surface wind observations may be analyzed to generate wind-frequency distributions by time-of-day categories (night, morning, afternoon and evening). Vertical turbulent intensities may be determined from a climatology of actual measurements or may be assigned on the basis of the Pasquill stability categories. Median mixing depths may be determined from the seasonal tabulations of the frequency of occurrence of wind speed and mixing depth. Vertical potential temperature gradients may be assigned to stability or time-of-day categories on the basis of climatology.

A.2 PLUME-RISE FORMULAS

The effective stack height H of a buoyant plume is given by the sum of the physical stack height h and the buoyant rise Δh. For an adiabatic or unstable atmosphere, the buoyant rise Δh_N is given by

$$\Delta h_N = \left[\frac{1}{\bar{u}\{h\}} \left(\frac{3F}{2\gamma_1^2} \right)^{1/3} (10h)^{2/3} \right] f \qquad \text{(A-1)}$$

TABLE A-2

METEOROLOGICAL INPUTS REQUIRED BY THE LONG-TERM CONCENTRATION MODEL

Parameter	Definition
$f_{i,j,k,\ell}$ (Table)	Frequency distribution of wind-speed and wind-direction categories by stability or time-of-day categories for the ℓ^{th} season
z_R	Height at which wind-frequency distributions were obtained
$p_{k,i}$ (Table)	Wind-profile exponents for each stability or time-of-day category and i^{th} wind-speed category
$\sigma'_{E;i,k}$ (Table)	Standard deviation of the wind-elevation angle in radians for the i^{th} wind-speed category and k^{th} stability or time-of-day category
$T_{a;k,\ell}$ (Table)	Ambient air temperature for the k^{th} stability or time-of-day category and ℓ^{th} season
$\left(\frac{\partial\theta}{\partial z}\right)_{i,k}$ (Table)	Vertical potential temperature gradient for the i^{th} wind-speed category and k^{th} stability or time-of-day category
$H_{m;i,k,\ell}$ (Table)	Median surface mixing depth for the i^{th} wind-speed category, k^{th} stability or time-of-day category and ℓ^{th} season
$\bar{u}\{z_R\}_i$ (Table)	Mean wind speeds at height z_R

where the expression in the brackets is from Briggs (1971; 1972) and

$\bar{u}\{h\}$ = the mean wind speed at the stack height h

γ_1 = the adiabatic entrainment coefficient ~ 0.6

F = the initial buoyancy flux

$$= \frac{gV}{\pi}\left(1 - \frac{T_a}{T_s}\right) \qquad \text{(A-2)}$$

V = the volumetric emission rate of the stack

$= \pi r^2 w$

r = inner radius of stack

w = stack exit velocity

g = the acceleration due to gravity

T_a = the ambient air temperature (^oK)

T_s = the stack exit temperature (^oK)

The factor f, which limits the plume rise as the mean wind speed at stack height approaches or exceeds the stack exit velocity, is defined by

$$f = \begin{cases} 1 & ; \quad \bar{u}\{h\} \leq w/1.5 \\ \left(\frac{3w - 3\bar{u}\{h\}}{w}\right) & ; \quad w/1.5 < \bar{u}\{h\} < w \\ 0 & ; \quad \bar{u}\{h\} \geq w \end{cases} \qquad \text{(A-3)}$$

The empirical correction factor f is generally not applied to stacks with Froude numbers less than about unity. The corresponding Briggs (1971) rise formula for a stable atmosphere (potential temperature gradient greater than zero) is

$$\Delta h_S = \left\{ \begin{array}{ll} \left[\dfrac{6F}{\bar{u}\{h\}\ \gamma_2^{\,2}\ S} \right]^{1/3} & ;\ \pi\ \bar{u}\{h\}\ S^{-1/2} < 10h \\ \left[\dfrac{3F}{\bar{u}\{h\}\ \gamma_2^{\,2}\ S} \left(1 - \cos\left(\dfrac{10 S^{1/2}\ h}{\bar{u}\{h\}} \right) \right) \right]^{1/3} & ;\ \pi\ \bar{u}\{h\}\ S^{-1/2} \geq 10h \end{array} \right\} f \quad \text{(A-4)}$$

where

γ_2 = the stable entrainment coefficient ~ 0.66

$S = \dfrac{g}{T_a} \dfrac{\partial \theta}{\partial z}$

$\dfrac{\partial \theta}{\partial z}$ = vertical potential temperature gradient

The entrainment coefficients γ_1 and γ_2 are based on the suggestions of Briggs (1972). It should be noted that Equation (A-4) does not permit the calculated stable rise Δh_s to exceed the adiabatic rise Δh_N as the atmosphere approaches a neutral stratification ($\partial\theta/\partial z$ approaches 0). A procedure of this type is recommended by Briggs (1972).

A.3 SHORT-TERM CONCENTRATION MODEL

A.3.1 Elevated Sources

The atmospheric dispersion model used to calculate hourly average ground-level concentrations downwind from an elevated continuous source is given by

$$\chi\{x, y\} = \frac{K\ Q}{\pi\ \bar{u}\{H\}\ \sigma_y\ \sigma_z} \{\text{Vertical Term}\}\ \{\text{Lateral Term}\}\ \{\text{Decay Term}\} \quad \text{(A-5)}$$

where

K = scaling coefficient to convert input parameters to dimensionally consistent units

Q = source emission rate

$\bar{u}\{H\}$ = mean wind speed at the plume stabilization height H

σ_y, σ_z = standard deviations of the lateral and vertical concentration distributions at downwind distance x

The Vertical Term refers to the plume expansion in the vertical or z direction and includes a multiple reflection term that limits cloud growth to the surface mixing layer.

$$\{\text{Vertical Term}\} = \left\{ \exp\left[-\frac{1}{2}\left(\frac{H}{\sigma_z}\right)^2 \right] + \sum_{n=1}^{\infty} \left[\exp\left[-\frac{1}{2}\left(\frac{2n\,H_m + H}{\sigma_z}\right)^2 \right] + \exp\left[-\frac{1}{2}\left(\frac{2n\,H_m - H}{\sigma_z}\right)^2 \right] \right] \right\} \tag{A-6}$$

where H_m is the depth of the surface mixing layer. The exponential terms in the infinite series in Equation (A-6) rapidly approach zero near the source. At the downwind distance where the exponential terms are non-zero for n equal 3, the plume has become approximately uniformly mixed within the surface mixing layer. In order to shorten computer computation time, Equation (A-6) is changed to the form

$$\{\text{Vertical Term}\} = \frac{\sqrt{2\pi}\,\sigma_z}{2H_m} \tag{A-7}$$

beyond this point. Equation (A-7) changes the form of the vertical concentration distribution from Gaussian to rectangular. If H exceeds H_m, the vertical term is set equal to zero which results in a zero value for the ground-level concentration.

The Lateral Term refers to the crosswind expansion of the plume and is given by the expression

$$\{\text{Lateral Term}\} = \exp\left[-\frac{1}{2}\left(\frac{y}{\sigma_y}\right)^2\right] \qquad \text{(A-8)}$$

where y is the crosswind distance from the plume centerline to the point at which concentration is calculated.

The Decay Term, which accounts for the possibility of pollutant removal by physical or chemical processes, is of the form

$$\{\text{Decay Term}\} = \exp\left[-\psi\, x/\bar{u}\{H\}\right] \qquad \text{(A-9)}$$

where

ψ = the washout coefficient Λ (sec^{-1}) for precipitation scavenging

= $\frac{0.692}{T_{1/2}}$, where $T_{1/2}$ is the pollutant half life for physical or chemical removal

= 0 for no depletion (ψ is automatically set to zero by the computer program unless otherwise specified)

In the model calculations, the observed mean wind speed $\bar{u}_R$ is adjusted from the measurement height z_R to the source height h for plume-rise calculations and to the stabilization height H for the concentration calculations by a wind-profile exponent law

$$\bar{u}\{z\} = \bar{u}\{z_R\}\left(\frac{z}{z_R}\right)^p \qquad \text{(A-10)}$$

The exponent p, which is assigned on the basis of atmospheric stability, ranges from about 0.1 for very unstable conditions to about 0.4 for very stable conditions.

According to the derivation in the report by Cramer, et al. (1972), the standard deviation of the lateral concentration distribution σ_y is given by the expression

$$\sigma_y\{x\} = \sigma'_A \, x_{ry} \left[\frac{x + x_y - x_{ry}(1-\alpha)}{\alpha x_{ry}} \right]^{\alpha} \qquad \text{(A-11)}$$

$$x_y = \begin{cases} \dfrac{\sigma_{yR}}{\sigma'_A} - x_R & ; \ \dfrac{\sigma_{yR}}{\sigma'_A} \leq x_{ry} \\ \alpha x_{ry} \left(\dfrac{\sigma_{yR}}{x_{ry}\, \sigma'_A} \right)^{1/\alpha} - x_R + x_{ry}(1-\alpha) & ; \ \dfrac{\sigma_{yR}}{\sigma'_A} > x_{ry} \end{cases} \qquad \text{(A-12)}$$

where

σ'_A = the standard deviation of the wind-azimuth angle in radians

x_{ry} = distance over which rectilinear plume expansion occurs downwind from an ideal point source ($\sim$ 50 meters)

σ_{yR} = the standard deviation of the lateral concentration distribution at downwind distance x_R

α = the lateral diffusion coefficient ($\sim$ 0.9)

The virtual distance x_y is not permitted to be less than zero. The lateral turbulent intensity σ'_A may be specified directly or may be assigned on the basis of the Pasquill stability category.

Following the derivation of Cramer, et al. (1972) and setting the vertical diffusion coefficient β equal to unity, the standard deviation of the vertical concentration distribution σ_z is given by the expression

$$\sigma_z\{x\} = \sigma'_E\left(x + x_z\right) \tag{A-13}$$

$$x_z = \left\{ \begin{array}{ll} \dfrac{\sigma_{zR}}{\sigma'_E} - x_R & ; \quad \dfrac{\sigma_{zR}}{\sigma'_E} \geq x_R \\ 0 & ; \quad \dfrac{\sigma_{zR}}{\sigma'_E} < x_R \end{array} \right\} \tag{A-14}$$

where

σ'_E = standard deviation of the wind-elevation angle in radians

σ_{zR} = the standard deviation of the vertical concentration distribution at downwind distance x_R

The vertical turbulent intensity σ'_E may also be obtained from direct measurements or may be assigned according to the Pasquill stability categories. When σ'_E values corresponding to the Pasquill stability categories are entered in Equation (A-13), the resulting curves will differ from the corresponding Pasquill-Gifford curves in that Equation (A-13) assumes rectilinear expansion at all downwind distances. Thus, σ_z values obtained from Equation (A-13) will be smaller than the values obtained from the Pasquill-Gifford A and B curves and larger than the values obtained from the D, E and F curves at long downwind distances. However, the multiple reflection term in Equation (A-6) which confines the plume to the surface mixing layer accounts for the behavior of the D, E and F curves (decrease in the expansion rate with distance) in a manner that may be related to the meteorology of the area.

Following the recommendations of Briggs (1972), the lateral and vertical standard deviations of a stabilized buoyant plume are defined by

$$\sigma_{yR} = \sigma_{zR} = \frac{0.5\,\Delta h}{2.15} \tag{A-15}$$

The downwind distance to stabilization x_R is given by

$$x_R = \left\{ \begin{array}{lll} 10h & ; & \frac{\partial \theta}{\partial z} \leq 0 \\ \pi \bar{u}\{h\} S^{-1/2} & ; & \frac{\partial \theta}{\partial z} > 0 \text{ and } \pi \bar{u}\{h\} S^{-1/2} < 10h \\ 10h & ; & \frac{\partial \theta}{\partial z} > 0 \text{ and } \pi \bar{u}\, h\, S^{-1/2} \geq 10h \end{array} \right\} \qquad \text{(A-16)}$$

A.3.2 Application of the Short-Term Model to Low-Level Emissions

The short-term diffusion model in Section A.3.1 may be used to calculate ground-level concentrations resulting from low-level emissions such as losses through building vents. These emissions are rapidly distributed by the cavity circulation of the building wake and quickly assume the dimensions of the building. Ground-level concentrations are calculated by setting the release height h and the buoyancy parameter F equal to zero. The standard deviation of the lateral concentration distribution at the source σ_{yo} is defined by the building crosswind dimension y_o divided by 4.3. The standard deviation of the vertical concentration distribution at the source σ_{zo} is obtained by dividing the building height by 2.15. The initial dimensions σ_{yo} and σ_{zo} are assumed to be applicable at the downwind edge of the building. It should be noted that separate turbulent intensities σ'_A and σ'_E may be defined for the low-level sources to account for the effects of surface roughness elements and heat sources.

A.3.3 Short-Term Concentration Model for Area Sources

The atmospheric dispersion model used to calculate ground-level concentrations at downwind distance x from the downwind edge of an area source is given by the expression

$$\chi\{x > x_o, y\} = \frac{K Q}{\sqrt{2\pi}\, u\{h\}\, \sigma_z\{x\}\, y_o} \{\text{Vertical Term}\}$$

$$\{\text{Lateral Term}\}\ \{\text{Decay Term}\} \qquad \text{(A-17)}$$

where

Q = area source strength in units of mass per unit time

y_o = crosswind source dimension

$$\sigma_z\{x\} = \left\{ \begin{array}{ll} \dfrac{\sigma'_E\, x_o}{\ln\left[\dfrac{\sigma'_E(x+x_o)+h}{\sigma'_E(x)+h}\right]} & ;\ x < 3x_o \\ \\ \sigma'_E(x+x_o/2)+h & ;\ x \geq 3x_o \end{array} \right\} \qquad \text{(A-18)}$$

x_o = alongwind dimension of the area source

h = the characteristic height of the area source

The Vertical Term for an area source is given by

$$\{\text{Vertical Term}\} = \left\{ \begin{array}{ll} 1+2\sum_{n=1}^{3}\left\{\exp\left[-\frac{1}{2}\left(\frac{2n\,H_m}{\sigma_z\{x\}}\right)^2\right]\right\} & ;\ \exp\left[-\frac{1}{2}\left(\frac{6H_m}{\sigma_z}\right)^2\right] = 0 \\ \\ \dfrac{\sqrt{2\pi}\,\sigma_z\{x\}}{2\,H_m} & ;\ \exp\left[-\frac{1}{2}\left(\frac{6H_m}{\sigma_z}\right)^2\right] > 0 \end{array} \right\} \qquad \text{(A-19)}$$

The Lateral Term is given by the expression

$$\{\text{Lateral Term}\} = \left\{ \text{erf}\left[\frac{y_o/2 + y}{\sqrt{2}\ \sigma_y\{x\}}\right] + \text{erf}\left[\frac{y_o/2 - y}{\sqrt{2}\ \sigma_y\{x\}}\right]\right\} \qquad \text{(A-20)}$$

where

y_o = crosswind dimension of the area source

y = crosswind distance from the centerline of the area source

and

$$\sigma_y\{x\} = \sigma'_A(x + x_o/2) \qquad \text{(A-21)}$$

The Decay Term is given by Equation (A-9) above.

The concentration at points interior to the area source is given by

$$\chi\{x'\} = \frac{2\,K\,Q}{\sqrt{2\pi}\ u\{h\}\ x_o\ y_o\ \sigma'_E}\left\{\ln\left[\frac{\sigma'_E(x' + 1) + h}{\sigma'_E + h}\right]\right\}\{\text{Vertical Term}\} \qquad \text{(A-22)}$$

where

x' = distance downwind from the upwind edge of the area source

A.4 LONG-TERM CONCENTRATION MODEL

A.4.1 Elevated Sources

The atmospheric dispersion model for elevated point and volume sources is similar in form to the Air Quality Display Model (Environmental Protection Agency, 1969) and the Climatological Dispersion Model (Calder, 1971). In the model, the area surrounding a continuous source of pollutants is divided into

sectors of equal angular width corresponding to the class intervals of the seasonal and annual frequency distributions of wind direction. The emission rate during a season or year is partitioned according to the relative wind-direction frequencies. Ground-level concentration fields for each source are translated to a common reference coordinate grid system and summed to obtain the total due to all emissions. For a single source, the mean seasonal concentration at a point (r, θ) is given by

$$\chi_{\ell}\{r,\theta\} = \frac{2KQ}{\sqrt{2\pi}\, r\, \Delta\theta'} \sum_{i,j,k} \left[\frac{f_{i,j,k,\ell}}{\bar{u}_i \{H_{i,k,\ell}\}\, \sigma_{z;i,k,\ell}} \; S\{\theta\} \; V_{i,k,\ell} \right. \tag{A-23}$$

$$\left. \exp\left[-\psi\, r/\bar{u}_i \{H_{i,k,\ell}\} \right] \right]$$

$$V_{i,k,\ell} = \exp\left[-\frac{1}{2}\left(\frac{H_{i,k,\ell}}{\sigma_{z;i,k,\ell}} \right)^2 \right] + \sum_{n=1}^{\infty} \left\{ \exp\left[-\frac{1}{2}\left(\frac{2n\, H_{m;i,k,\ell} - H_{i,k,\ell}}{\sigma_{z;i,k,\ell}} \right)^2 \right] \right. \tag{A-24}$$

$$\left. + \exp\left[-\frac{1}{2}\left(\frac{2n\, H_{m;i,k,\ell} + H_{i,k,\ell}}{\sigma_{z;i,k,\ell}} \right)^2 \right] \right\}$$

where

$f_{i,j,k,\ell}$ = frequency of occurrence of the i^{th} wind-speed category, j^{th} wind-direction category and k^{th} stability or time-of-day category for the ℓ^{th} season

$\Delta\theta'$ = the sector width in radians

$S\{\theta\}$ = a smoothing function

$$S\{\theta\} = \begin{cases} \dfrac{\Delta\theta' - \left|\theta'_j - \theta'\right|}{\Delta\theta'} & ; \quad \left|\theta'_j - \theta'\right| \leq \Delta\theta' \\ 0 & ; \quad \left|\theta'_j - \theta'\right| > \Delta\theta' \end{cases} \qquad \text{(A-25)}$$

θ'_j = the angle measured in radians from north to the centerline of the j^{th} wind-direction sector

θ' = the angle measured in radians from north to the point (r, θ)

As with the short-term model, the Vertical Term given by Equation (A-24) is changed to the form

$$V_{i,k,\ell} = \frac{\sqrt{2\pi}\ \sigma_{z;i,k,\ell}}{2H_{m;i,k,\ell}} \qquad \text{(A-26)}$$

when the exponential terms in Equation (A-24) become non-zero for n equal 3. The remaining terms in Equations (A-23) and (A-24) are identical to those previously defined in Section A.3.1 for the short-term model, except that the turbulent intensities and potential temperature gradients may be separately assigned to each wind-speed and/or stability (or time-of-day) category; the ambient air temperatures may be separately assigned to each stability (or time-of-day) category for each season; and the surface mixing depths may be separately assigned to each wind-speed and/or stability (or time-of-day) category for each season.

As shown by Equation (A-25), the rectangular concentration distribution within a given angular sector is modified by the function $S\{\theta\}$ which smoothes discontinuities in the concentration at the boundaries of adjacent sectors. The centerline concentration in each sector is unaffected by contributions from adjacent sectors. At points off the sector centerline, the concentration is a weighted

function of the concentration at the centerline of the sector in which the calculation is being made and the concentration at the centerline of the nearest adjoining sector.

The mean annual concentration at the point (r, θ) is calculated from the seasonal concentrations using the expression

$$\chi_a\{r, \theta\} = \frac{1}{4} \sum_{\ell} \chi_{\ell} \{r, \theta\} \qquad \text{(A-27)}$$

A.4.2 Application of the Long-Term Model to Low-Level Emissions

Long-term ground-level concentrations produced by low-level emissions are calculated from Equation (A-23) by setting the source height h and the buoyancy parameter F equal to zero. The standard deviation of the vertical concentration distribution at the downwind edge of the building σ_{zo} is defined as the building height divided by 2.15. Separate vertical turbulent intensities σ'_E may be defined for the low-level sources to account for the effects of surface heat sources and roughness elements. A virtual point source is used to account for the initial lateral dimension of the source in a manner identical to that described below for area sources.

A.4.3 Long-Term Concentration Model for Area Sources

The mean seasonal concentration at downwind distance r with respect to the center of an area source is given by the expression

$$\chi_{\ell}\{r > r_o\} = \frac{2KQ}{\sqrt{2\pi}\, R\, \Delta\theta} \left\{ \sum_{i,j,k} \left[\frac{f_{i,j,k,\ell}}{\bar{u}_i\{h\}_{z;i,k}} \; S\{\theta\} \; V_{i,k,\ell} \right] \right\} \tag{A-28}$$

$$\exp\left[- \psi (r' - r_o) / \bar{u}_i\{h\} \right]$$

where

R = radial distance from the virtual point source to the receptor

$$= \left((r' + x_y)^2 + y^2 \right)^{1/2}$$

r' = distance from source center to receptor, measured along the plume axis

r_o = effective source radius

y = lateral distance from the cloud axis to the receptor

x_y = virtual distance

$$= r_o \cot \frac{\Delta\theta'}{2} \tag{A-29}$$

$$\sigma_{z;i,k} = \left\{ \begin{array}{ll} \dfrac{2\sigma'_{E;i,k}\, r_o}{\ln \left[\dfrac{\sigma'_{E;i,k}(r' + r_o) + h}{\sigma'_{E;i,k}(r' - r_o) + h} \right]} & ; \quad r_o < r' < 6r_o \\ \\ \sigma'_{E;i,k}\, r' + h & ; \quad r' \geq 6r_o \end{array} \right\} \tag{A-30}$$

$$V_{i,k,\ell} = \begin{cases} 1 + 2\sum_{n=1}^{3} \exp\left[-\frac{1}{2}\left(\frac{2n\,H_{m;i,k,\ell}}{\sigma_{z;i,k}}\right)^2\right]; \exp\left[-\frac{1}{2}\left(\frac{6H_{m;i,k,\ell}}{\sigma_{z;i,k}}\right)^2\right] = 0 \\ \frac{\sqrt{2\pi}\,\sigma_{z;i,k}}{2H_{m;i,k,\ell}} \quad ; \exp\left[-\frac{1}{2}\left(\frac{6H_{m;i,k,\ell}}{\sigma_{z;i,k}}\right)^2\right] > 0 \end{cases} \quad \text{(A-31)}$$

and the remaining parameters are identical to those previously defined.

For points interior to the area source, the concentration for seasonal models is given by the expression

$$\chi_\ell\{r \le r_o\} = \frac{2KQ}{\sqrt{2\pi}\,x_o\,y_o} \sum_{i,j,k} \left[\frac{f_{i,j,k,\ell}}{\bar{u}_i\{h\}\,\sigma'_{E;i,k}} \ln\left[\frac{\sigma'_{E;i,k}(r'' + 1) + h}{\sigma'_{E;i,k} + h}\right] V_{i,k,\ell}\right] \quad \text{(A-32)}$$

where

r'' = the downwind distance, measured along the plume axis from the upwind edge of the area source

A.5 APPLICATION OF THE SHORT-TERM AND LONG-TERM CONCENTRATION MODELS IN COMPLEX TERRAIN

The short-term and long-term concentration models described in Sections A.3 and A.4 are strictly applicable only for flat terrain where the base of the stack (or the building source) and the ground surface downwind from the source are at the same elevation. However, both models may also be applied to complex terrain by defining effective stabilization heights and mixing depths. The following assumptions are made in the model calculations for complex terrain:

- The top of the surface mixing layer extends over the calculation grid at a constant height above mean sea level

- Ground-level concentrations at all grid points above the top of the surface mixing layer are zero

- Plumes that stabilize above the top of the surface mixing layer do not contribute to ground-level concentrations at any grid point (this assumption also applies to flat terrain)

In order to determine whether the stabilized plume is contained within the surface mixing layer, it is necessary to calculate the mixing depth $H_m^*\{z_s\}$ at the source from the relationship

$$H_m^*\{z_s\} = \left(H_m + z_a - z_s\right) \qquad \text{(A-33)}$$

where

H_m = the depth of the surface mixing layer measured at a point with elevation z_a above mean sea level

z_s = the height above mean sea level of the source

Equation (A-33) is represented schematically in Figure A-1. As shown by the figure, the actual top of the surface mixing layer is assumed to remain at a constant elevation above mean sea level. If the height H of the stabilized plume above the base of the stack is less than or equal to $H_m^*\{z_s\}$, the plume is defined to be contained within the surface mixing layer.

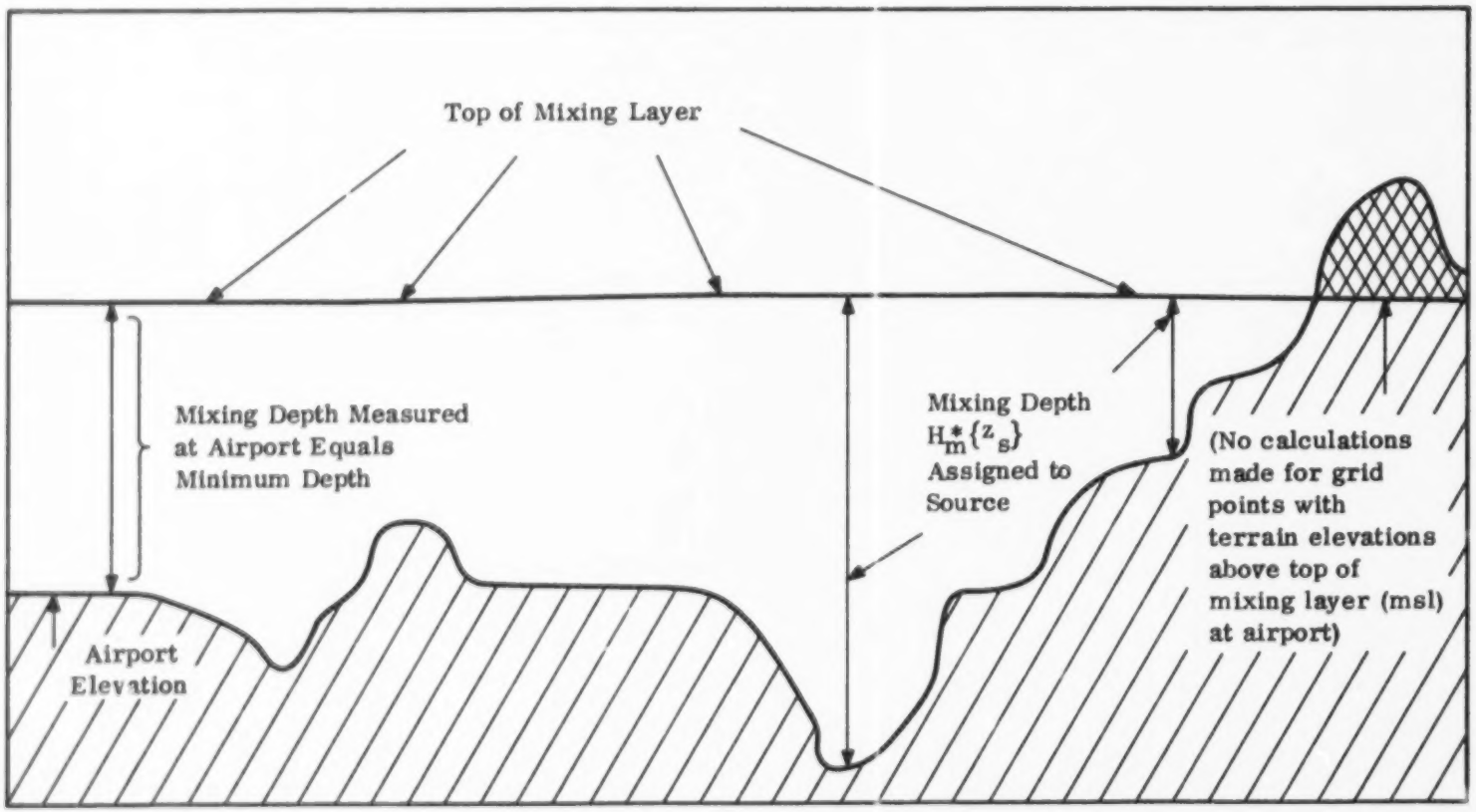
Top of Mixing Layer
Mixing Depth Measured at Airport Equals Minimum Depth
Airport Elevation
Mixing Depth $H_m^*\{z_s\}$ Assigned to Source
(No calculations made for grid points with terrain elevations above top of mixing layer (msl) at airport)

FIGURE A-1. Mixing depth $H_m^*\{z_s\}$ used to determine whether the stabilized plume is contained within the surface mixing layer.

The height H_o of the stabilized plume above mean sea level is given by the sum of the height H of the stabilized plume above the base of the stack and the elevation z_s of the base of the stack. At any elevation z above mean sea level, the effective height $H'\{z\}$ of the plume centerline above the terrain is then given by

$$H'\{z\} = \begin{cases} H_o - z & ; \; H_o - z \geq 0 \\ 0 & ; \; H_o - z < 0 \end{cases} \qquad \text{(A-34)}$$

For building sources, $H'\{z\}$ is always set equal to zero.

The effective mixing depth $H_m'\{z\}$ above a point at elevation z above mean sea level is defined by

$$H_m'\{z\} = \begin{cases} H_m & ; \; z \geq z_a \\ H_m + z_a - z & ; \; z < z_a \end{cases} \qquad \text{(A-35)}$$

Figure A-2 illustrates the assumptions implicit in Equation (A-35). For grid points at elevations below the airport elevation, the effective mixing depth $H_m'\{z\}$ is allowed to increase in a manner consistent with Figure A-1. However, in order to prevent a physically unrealistic compression of plumes as they pass over elevated terrain, the effective mixing depth is not permitted to be less than the mixing depth measured at the airport. It should be noted that the concentration is set equal to zero for grid points above the actual top of the mixing layer (see Figure A-1).

The terrain adjustment procedures also assume that the mean wind speed at any given height above sea level is constant. Thus, the wind speed $\bar{u}_R$ measured at height z_R above the surface at a point with elevation z_a above mean

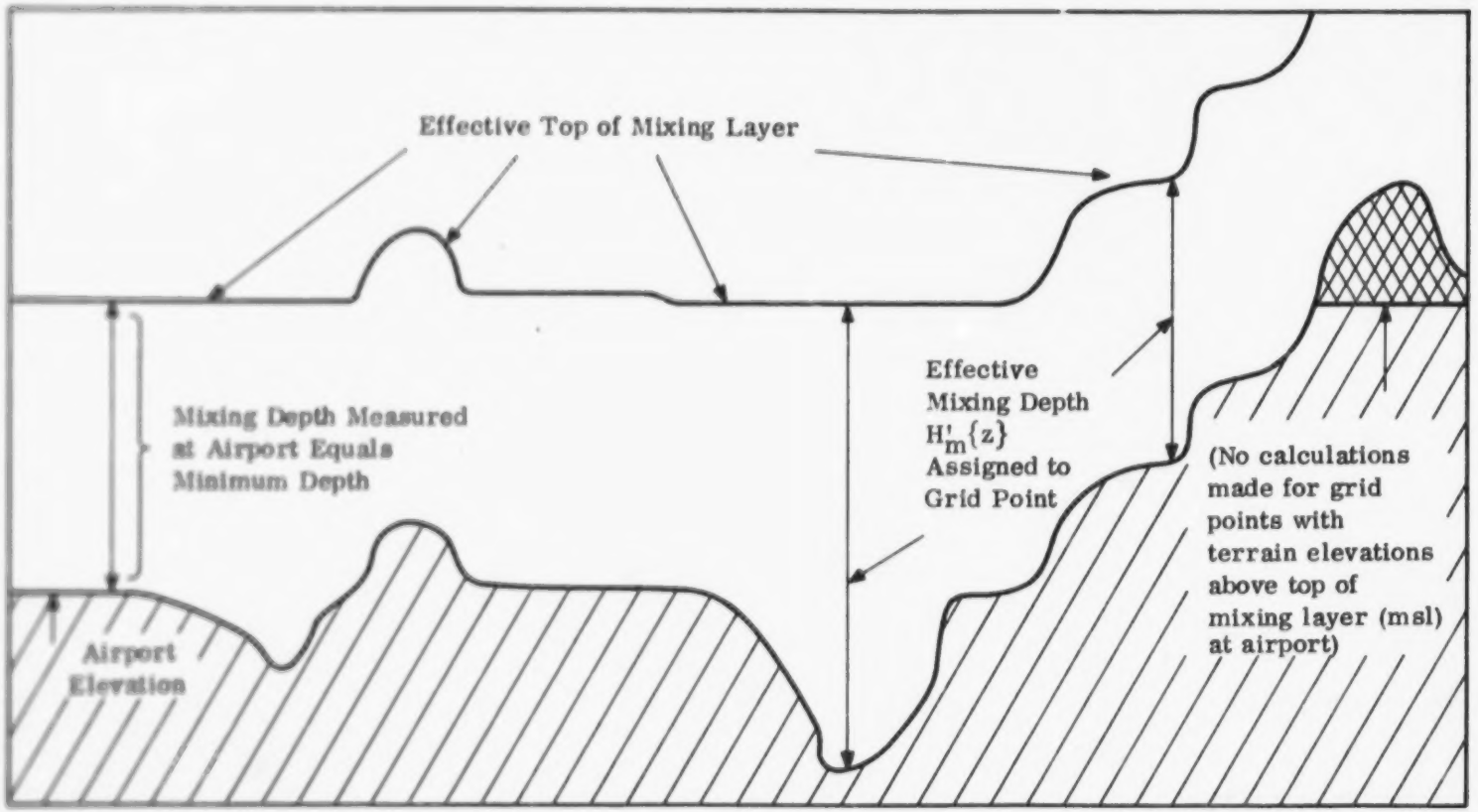
Effective Top of Mixing Layer
Mixing Depth Measured at Airport Equals Minimum Depth
Effective Mixing Depth $H'_m\{z\}$ Assigned to Grid Point
(No calculations made for grid points with terrain elevations above top of mixing layer (msl) at airport)
Airport Elevation

FIGURE A-2. Effective mixing depth $H'_m\{z\}$ assigned to grid points for the concentration calculations.

sea level is adjusted to the stack height for the plume-rise calculations by the relationship

$$\bar{u}\{h\} = \left\{ \begin{array}{ll} \bar{u}_R \left(\dfrac{h_o - z_a}{z_R} \right)^p & ; \quad h_o \geq z_a + z_R \\ \\ \bar{u}_R & ; \quad h_o < z_a + z_R \end{array} \right\} \qquad \text{(A-36)}$$

where h_o is the height above mean sea level of the top of the stack. Similarly, the wind speed $\bar{u}\{H\}$ used in the concentration calculations is given by

$$\bar{u}\{H\} = \left\{ \begin{array}{ll} \bar{u}_R \left(\dfrac{H_o - z_a}{z_R} \right)^p & ; \quad H_o \geq z_a + z_R \\ \\ \bar{u}_R & ; \quad H_o < z_a + z_R \end{array} \right\} \qquad \text{(A-37)}$$

It should be noted that the terrain-adjustment procedures outlined above provide a very simple representation of complex plume-terrain interactions that are not yet well understood. Because the model assumptions are generally conservative, it is possible that concentrations calculated for elevated terrain, especially elevated terrain near a source, exceed the concentrations that actually occur. It should also be noted that the procedures described above differ from previous "terrain-intersection" models in that terrain intersection is only permitted for a plume contained within a mixing layer. That is, terrain intersection is permitted for all stability categories, but only for a plume contained within the surface mixing layer.

APPENDIX B

ANNUAL FREQUENCY DISTRIBUTION OF WIND SPEED AND WIND DIRECTION AT THE GREATER PITTSBURGH AIRPORT

Tables B-1 through B-6 list the annual joint frequency of occurrence by Pasquill stability category of wind-speed and wind-direction categories at the Greater Pittsburgh Airport for the period 1963 through 1972. These distributions were developed by the STAR program of the National Climatic Center which uses the Turner (1964) definitions of the Pasquill stability categories.

TABLE B-1

ANNUAL FREQUENCY OF OCCURRENCE OF WIND SPEED AND WIND DIRECTION AT THE GREATER PITTSBURGH AIRPORT FOR THE A STABILITY CATEGORY DURING THE PERIOD 1963 THROUGH 1972

Direction (Sector)	Wind Speed (meters per second)						
	00.0-01.5	01.6-03.0	03.1-05.1	05.2-08.2	08.3-10.8	> 10.8	Total
N	.0063	.0171	.0000	.0000	.0000	.0000	.0234
NNE	.0107	.0098	.0000	.0000	.0000	.0000	.0205
NE	.0053	.0122	.0000	.0000	.0000	.0000	.0176
ENE	.0107	.0098	.0000	.0000	.0000	.0000	.0205
E	.0068	.0196	.0000	.0000	.0000	.0000	.0263
ESE	.0029	.0147	.0000	.0000	.0000	.0000	.0176
SE	.0048	.0245	.0000	.0000	.0000	.0000	.0293
SSE	.0058	.0147	.0000	.0000	.0000	.0000	.0205
S	.0029	.0147	.0000	.0000	.0000	.0000	.0176
SSW	.0034	.0171	.0000	.0000	.0000	.0000	.0205
SW	.0024	.0122	.0000	.0000	.0000	.0000	.0146
WSW	.0062	.0318	.0000	.0000	.0000	.0000	.0380
W	.0044	.0073	.0000	.0000	.0000	.0000	.0117
WNW	.0034	.0024	.0000	.0000	.0000	.0000	.0059
NW	.0034	.0171	.0000	.0000	.0000	.0000	.0205
NNW	.0014	.0073	.0000	.0000	.0000	.0000	.0088
Total	.0807	.2324	.0000	.0000	.0000	.0000	.3132

TABLE B-2

ANNUAL FREQUENCY OF OCCURRENCE OF WIND-SPEED AND WIND-DIRECTION AT THE GREATER PITTSBURGH AIRPORT FOR THE B STABILITY CATEGORY DURING THE PERIOD 1963 THROUGH 1972

Direction (Sector)	Wind Speed (meters per second)						
	00.0-01.5	01.6-03.0	03.1-05.1	05.2-08.2	08.3-10.8	> 10.8	Total
N	.0541	.1370	.1150	.0000	.0000	.0000	.3061
NNE	.0493	.0905	.0612	.0000	.0000	.0000	.2009
NE	.0611	.1101	.0294	.0000	.0000	.0000	.2005
ENE	.0545	.1052	.0563	.0000	.0000	.0000	.2160
E	.0989	.1835	.0881	.0000	.0000	.0000	.3705
ESE	.0765	.1174	.0612	.0000	.0000	.0000	.2551
SE	.0880	.1174	.0440	.0000	.0000	.0000	.2494
SSE	.0855	.1199	.0538	.0000	.0000	.0000	.2592
S	.1100	.1468	.1297	.0000	.0000	.0000	.3864
SSW	.0517	.0881	.0709	.0000	.0000	.0000	.2107
SW	.0574	.1052	.1028	.0000	.0000	.0000	.2654
WSW	.0790	.1492	.0856	.0000	.0000	.0000	.3138
W	.0753	.1101	.1150	.0000	.0000	.0000	.3004
WNW	.0509	.1003	.0538	.0000	.0000	.0000	.2050
NW	.0484	.0856	.0538	.0000	.0000	.0000	.1879
NNW	.0432	.0538	.0881	.0000	.0000	.0000	.1851
Total	1.0838	1.8202	1.2086	.0000	.0000	.0000	4.1126

TABLE B-3

ANNUAL FREQUENCY OF OCCURRENCE OF WIND SPEED AND WIND DIRECTION AT THE GREATER PITTSBURGH AIRPORT FOR THE C STABILITY CATEGORY DURING THE PERIOD 1963 THROUGH 1972

Direction (Sector)	Wind Speed (meters per second)						
	00.0-01.5	01.6-03.0	03.1-05.1	05.2-08.2	08.3-10.8	> 10.8	Total
N	.0457	.1688	.4208	.0563	.0000	.0000	.6916
NNE	.0323	.1052	.1737	.0196	.0000	.0000	.3308
NE	.0341	.1199	.2055	.0122	.0000	.0000	.3718
ENE	.0295	.1713	.2471	.0122	.0000	.0000	.4601
E	.0616	.1859	.2544	.0367	.0000	.0000	.5387
ESE	.0583	.1370	.2422	.0171	.0000	.0000	.4546
SE	.0998	.2275	.2104	.0245	.0024	.0000	.5646
SSE	.0561	.1859	.2471	.0098	.0000	.0000	.4989
S	.0811	.2765	.4208	.0343	.0000	.0000	.8126
SSW	.0341	.1419	.2936	.0563	.0024	0000	.5283
SW	.0515	.1933	.4966	.0954	.0024	.0024	.8417
WSW	.0506	.1859	.5823	.0783	.0098	.0049	.9118
W	.0411	.2202	.4918	.1639	.0122	.0024	.9316
WNW	.0528	.1590	.3914	.0416	.0147	.0049	.6644
NW	.0195	.1125	.3058	.0954	.0049	.0000	.5381
NNW	.0103	.0832	.2716	.0489	.0000	.0000	.4140
Total	.7584	2.6741	5.2552	.8025	.0489	.0147	9.5538

TABLE B-4

ANNUAL FREQUENCY OF OCCURRENCE OF WIND SPEED AND WIND DIRECTION AT THE GREATER PITTSBURGH AIRPORT FOR THE D STABILITY CATEGORY DURING THE PERIOD 1963 THROUGH 1972

Direction (Sector)	Wind Speed (meters per second)						
	00.0-01.5	01.6-03.0	03.1-05.1	05.2-08.2	08.3-10.8	> 10.8	Total
N	.0888	.6483	1.7982	1.2208	.0391	.0000	3.7954
NNE	.0787	.4355	.6801	.2544	.0073	.0000	1.4561
NE	.1120	.5333	.5896	.1517	.0024	.0000	1.3891
ENE	.0549	.3963	.7633	.2814	.0220	.0024	1.5204
E	.1031	.5921	.9737	.2740	.0147	.0000	1.9576
ESE	.1024	.5823	.9884	.4306	.0147	.0000	2.1184
SE	.1100	.6875	1.1205	.4184	.0147	.0049	2.3560
SSE	.1225	.5333	.7853	.2667	.0049	.0000	1.7128
S	.1689	.8490	1.4508	.6655	.0391	.0073	3.1806
SSW	.0724	.4208	1.2771	.9590	.0807	.0049	2.8150
SW	.1172	.6410	2.0404	2.5835	.3229	.0416	5.7467
WSW	.1238	.5872	2.1040	3.3322	.8392	.2373	7.2236
W	.1323	.7780	2.3731	4.0539	.9884	.2838	8.6096
WNW	.0904	.4526	1.3603	2.5664	.6288	.0954	5.1939
NW	.0870	.4771	1.4630	1.8520	.3572	.0416	4.2779
NNW	.0380	.2716	1.2477	1.4361	.1052	.0122	3.1109
Total	1.6025	8.8858	21.0158	20.7467	3.4814	.7315	56.4638

TABLE B-5

ANNUAL FREQUENCY OF OCCURRENCE OF WIND SPEED AND WIND DIRECTION AT THE GREATER PITTSBURGH AIRPORT FOR THE E STABILITY CATEGORY DURING THE PERIOD 1963 THROUGH 1972

Direction (Sector)	Wind Speed (meters per second)						
	00.0-01.5	01.6-03.0	03.1-05.1	05.2-08.2	08.3-10.8	> 10.8	Total
N	.0000	.3988	.7291	.0000	.0000	.0000	1.1279
NNE	.0000	.3107	.2447	.0000	.0000	.0000	.5554
NE	.0000	.3621	.1810	.0000	.0000	.0000	.5431
ENE	.0000	.3205	.1639	.0000	.0000	.0000	.4844
E	.0000	.6459	.1028	.0000	.0000	.0000	.7486
ESE	.0000	.5945	.2202	.0000	.0000	.0000	.8147
SE	.0000	.6655	.1297	.0000	.0000	.0000	.7951
SSE	.0000	.5211	.1150	.0000	.0000	.0000	.6361
S	.0000	.7217	.1786	.0000	.0000	.0000	.9003
SSW	.0000	.4991	.2324	.0000	.0000	.0000	.7315
SW	.0000	.5921	.5285	.0000	.0000	.0000	1.1205
WSW	.0000	.3988	.5431	.0000	.0000	.0000	.9419
W	.0000	.4233	.6459	.0000	.0000	.0000	1.0691
WNW	.0000	.3401	.3009	.0000	.0000	.0000	.6410
NW	.0000	.2911	.3890	.0000	.0000	.0000	.6801
NNW	.0000	.1443	.4746	.0000	.0000	.0000	.6190
Total	.0000	7.2295	5.1793	.0000	.0000	.0000	12.4089

TABLE B-6

ANNUAL FREQUENCY OF OCCURRENCE OF WIND SPEED AND WIND DIRECTION AT THE GREATER PITTSBURGH AIRPORT FOR THE F STABILITY CATEGORY DURING THE PERIOD 1963 THROUGH 1972

Direction (Sector)	Wind Speed (meters per second)						
	00.0-01.5	01.6-03.0	03.1-05.1	05.2-08.2	08.3-10.8	> 10.8	Total
N	.4758	.6850	.0000	.0000	.0000	.0000	1.1608
NNE	.4145	.5040	.0000	.0000	.0000	.0000	.9185
NE	.4716	.4722	.0000	.0000	.0000	.0000	.9438
ENE	.4219	.3303	.0000	.0000	.0000	.0000	.7522
E	.7206	.5921	.0000	.0000	.0000	.0000	1.3127
ESE	.6315	.4208	.0000	.0000	.0000	.0000	1.0523
SE	.6735	.4330	.0000	.0000	.0000	.0000	1.1065
SSE	.5093	.2862	.0000	.0000	.0000	.0000	.7956
S	.9581	.5896	.0000	.0000	.0000	.0000	1.5477
SSW	.3745	.3523	.0000	.0000	.0000	.0000	.7268
SW	.5858	.4991	.0000	.0000	.0000	.0000	1.0848
WSW	.5325	.5162	.0000	.0000	.0000	.0000	1.0487
W	.9510	.8269	.0000	.0000	.0000	.0000	1.6779
WNW	.6406	.6214	.0000	.0000	.0000	.0000	1.2620
NW	.6334	.6214	.0000	.0000	.0000	.0000	1.2548
NNW	.2188	.2838	.0000	.0000	.0000	.0000	.5026
Total	9.1134	8.0344	.0000	.0000	.0000	.0000	17.1478

APPENDIX C

COMPARISON OF CALCULATED AND OBSERVED PLUME CHARACTERISTICS FOR THE MITCHELL AND KAMMER POWER PLANTS

C.1 BACKGROUND

During the period 25 August 1975 through 12 September 1975, the Environmental Monitoring and Support Laboratory (EMSL) of the U. S. Environmental Protection Agency made airborne measurements of SO_2 concentrations downwind from the Mitchell and Kammer Power Plants (Johnson, et al., 1976). As a test of the short-term diffusion model and modeling procedures used in this study, we used concurrent meteorological and emissions data for the various EMSL trials to calculate short-term plume characteristics (stabilization heights, axial concentrations and maximum short-term ground-level concentrations on elevated terrain) for comp. rison with the ground-level concentrations and plume cross-sections obtained by EMSL.

It should be noted that, in order to calculate axial concentrations, it was necessary to modify the short-term diffusion model described in Section A.3 of Appendix A. Specifically, a generalized Vertical Term was substituted for the ground-level Vertical Term given by Equation (A-6). The generalized Vertical Term is given by

$$\text{(Vertical Term)} = \frac{1}{2}\left\{\exp\left[-\frac{1}{2}\left(\frac{H-z}{\sigma_z}\right)^2\right] + \exp\left[-\frac{1}{2}\left(\frac{H+z}{\sigma_z}\right)^2\right]\right.$$
$$+ \sum_{n=1}^{\infty}\left[\exp\left[-\frac{1}{2}\left(\frac{2n\,H_m + H + z}{\sigma_z}\right)^2\right] + \exp\left[-\frac{1}{2}\left(\frac{2n\,H_m + H - z}{\sigma_z}\right)^2\right]\right. \quad \text{(C-1)}$$
$$\left.\left. + \exp\left[-\frac{1}{2}\left(\frac{2n\,H_m - H + z}{\sigma_z}\right)^2\right] + \exp\left[-\frac{1}{2}\left(\frac{2n\,H_m - H - z}{\sigma_z}\right)^2\right]\right]\right\}$$

where z is the height above the surface and the remaining terms in Equation (C-1) are defined in Appendix A.

C.2 EMISSIONS DATA FOR THE EMSL TRIALS

Table C-1 lists, for each trial, the volumetric and SO_2 emission rates for each power plant stack. As shown by the table, emissions parameters for both plants varied significantly from trial to trial. During most of the trials, the Mitchell plant was operating at about ten percent of its capacity, resulting in a stack exit velocity of about three meters per second. However, exit-velocity restrictions on plume rise (see Equation (A-3) of Appendix A) were not assumed to apply because the Froude number of the Mitchell stack during these trials was much less than unity.

C.3 METEOROLOGICAL DATA FOR THE EMSL TRIALS

Table C-2 lists the meteorological input parameters for the trials included in our analysis (the reasons for deleting several trials from our analysis are given below). When possible, the vertical potential temperature gradient $\partial\theta/\partial z$ and the mixing depth H_m were obtained from EMSL helicopter temperature soundings made during the trials. In the absence of helicopter temperature soundings, or if these soundings did not extend through a sufficiently deep layer, synoptic upper-air soundings made at the Greater Pittsburgh Airport were used to estimate these parameters. For each trial, the wind-profile exponent p was obtained by fitting a logarithmic least-squares curve to the average of the wind speeds measured by the synoptic upper-air sounding before and after the trial (a detailed description of this procedure is given in Section 3 of Cramer, et al., 1975). The average surface wind speeds during each trial at the Greater Pittsburgh and Wheeling, West Virginia Airports were adjusted to the two stack heights using these wind-

TABLE C-1

AVERAGE VOLUMETRIC AND SO_2 EMISSION RATES FOR THE MITCHELL AND KAMMER POWER PLANTS DURING THE TIME PERIODS OF THE EMSL TRIALS

Trial No.	Date (1975)	Time (EST)	Volumetric Emission Rates (m^3/sec)			SO_2 Emission Rates (g/sec)		
			Mitchell	Kammer No. 1	Kammer No. 2	Mitchell	Kammer No. 1	Kammer No. 2
1	25 Aug	0739-0921	185.1	634.9	314.9	3,771	3,309	1,660
2	26 Aug	0859-0959	193.4	634.9	339.2	4,772	2,853	1,431
3	27 Aug	1005-1316	204.9	648.9	339.2	1,961	3,359	1,684
4	28 Aug	0914-1217	Down	664.5	335.7	-0-	3,435	1,722
5	28 Aug	1430-1655	Down	678.4	341.0	-0-	3,435	1,722
6	29 Aug	0750-1107	Down	673.2	*	-0-	3,831	364
7	2 Sep	1024-1320	244.6	688.9	299.2	4,068	3,010	1,509
8	3 Sep	0919-1234	254.5	661.0	339.2	5,208	2,989	1,499
9	3 Sep	1350-1531	250.2	692.3	341.0	5,208	2,989	1,499
10	4 Sep	1215-1444	266.1	300.9	339.2	5,704	2,175	1,557
11	5 Sep	0930-1245	277.7	313.1	344.4	5,879	1,819	1,819
12	8 Sep	0905-1247	309.1	669.7	Down	4,486	2,262	-0-
13	9 Sep	0817-0852	1,717.2	624.0	Down	8,343	3,854	-0-
14	9 Sep	1027-1331	1,718.9	661.0	Down	8,343	3,854	-0-
15	10 Sep	0924-1255	1,740.4	629.7	280.1	11,214	2,676	1,342
16	11 Sep	0831-1109	1,763.5	666.2	351.4	10,720	3,216	1,613
17	11 Sep	1243-1336	1,765.1	685.4	354.9	10,720	3,216	1,613

* Stack went down during trial.

TABLE C-2

METEOROLOGICAL INPUT PARAMETERS

Trial No.	Pasquill Stability Category	$\bar{u}$ {h} (m/sec)		T_a	H_m	$\frac{\partial \theta}{\partial z}$	p	σ'_A	σ'_E
		Mitchell	Kammer	(^oK)	(m)	(^oK/m)		(rad)	(rad)
1	C	4.8	N/A	298.6	530	0.003	0.126	0.0100	0.0100
3	B	4.4	2.4	299.0	1954	0.001	0.217	0.1080	0.1080
5	C	N/A	3.5	302.1	3045	0.000	0.161	0.0735	0.0735
6	D	N/A	4.0	297.0	750	0.004	0.173	0.0465	0.0465
7	D	7.3	5.1	296.7	2000	0.000	0.130	0.0465	0.0465
8	B	7.1	3.2	292.1	567	0.000	0.289	0.0100	0.0100
10	D	N/A	5.0	298.9	745	0.000	0.207	0.0465	0.0465
11	B	7.3	4.0	295.3	705	0.000	0.274	0.1080	0.1080
12	C	10.3	5.5	296.1	440	0.000	0.238	0.0100	0.0100
13	D	5.2	3.8	296.1	1105	0.005	0.263	0.0465	0.0465
15	B	3.9	2.9	291.9	745	0.003	0.114	0.1080	0.1080
16*	C-D	10.5	6.2	295.3	325	0.009	0.194	0.0100	0.0100
17	D	N/A	4.4	296.5	3150	0.003	0.244	0.0465	0.0465

*Meteorological conditions during this trial rapidly changed to those given for Trial 17.

profile exponents (see Equation (A-36 of Appendix A). For some of the trials, EMSL estimated average wind speeds at the stack heights by averaging the wind speeds obtained from single-theodolite Pibal soundings. Calculations were performed for each of the three wind speeds; the wind speeds in Table C-2 are the wind speeds that yielded the best correspondence between calculated and observed plume rises and/or concentrations. The ambient air temperatures T_a in Table C-2 are the average temperatures measured at the Wheeling Airport during each trial. Also, the Wheeling Airport surface weather observations during each trial were used to assign the Pasquill stability category following the Turner (1964) procedures (see Section 2.2). With the exception of the trials with plume stabilization heights above the top of the surface mixing layer, the ten-minute lateral (σ'_A) and vertical (σ'_E) turbulent intensities given in Table C-2 for each trial correspond to the appropriate stability category (see Section 2.2). Lateral and vertical turbulent intensities in an elevated stable layer were assumed to be minimal (0.01 radians).

C.4 RESULTS OF THE ANALYSIS

The interpretation of aircraft measurements of plume characteristics is usually complicated by one or more of the following factors:

- The meteorological conditions or source emissions parameters may change during a trial (near steady-state conditions are required if the trial is to be used for model validation)
- There is frequently some uncertainty about the exact orientation of the aircraft with respect to the plume axis (i.e., the flight path may not be normal to the plume axis)

- It is difficult to assign the proper averaging time to observed concentrations and plume dimensions, expecially when multiple traverses are made at a fixed downwind distance

The Mitchell and Kammer trials were further complicated by the superposition of two or more plumes and the presence of other SO_2 sources in the area that contributed to a background SO_2 concentration of 0.01 to 0.05 parts per million (ppm). Thus, not all of the trials were suitable for model validation. For these reasons, we restricted our analysis of the EMSL data to the least ambiguous parameters: plume rise, axial concentrations and ground-level concentrations on elevated terrain. The validity of our assumptions about lateral and vertical plume growth was inferfed from the correspondence between calculated and observed concentrations.

Plume Rise

The observed plume rise for each stack was determined for each trial by subtracting the stack height from the height of the corresponding maximum observed SO_2 concentration at the closest downwind distance at which aircraft measurements were made. This measurement distance was always greater than the plume stabilization distance calculated from Equation (A-16) and was also frequently at a distance where the plume from the Kammer No. 2 stack was significantly affected by reflection from the ground. In these cases, the height of the maximum observed SO_2 concentration for the Kammer No. 2 plume should be lower than the plume stabilization height because reflection from the ground decreases the height of the maximum concentration and eventually brings it to the ground surface. Reflection from the bases of elevated inversions at the top of the surface mixing layer also affected the observed SO_2 concentrations in some of the trials, but this effect was generally small in comparison with the effect of ground reflection. Interaction of the Kammer No. 1 and No. 2 plumes additionally affected the observed

maximum concentrations and introduced other uncertainties in the determination of the observed plume rises from the aircraft measurements.

Table C-3 shows the observed plume rises determined from the aircraft measurements and the corresponding plume rises calculated from the Briggs (1971; 1972) equations. For the reasons given above, we believe that the observed plume rises for the Kammer No. 2 stack generally underestimate the actual plume rises and have indicated this qualification by quotation marks. In Trials 10 and 11, the heat contents and SO_2 emissions for both Kammer plumes were nearly identical and the aircraft observations for each trial showed a single merged plume.

The calculated and observed plume rises in Table C-3 are compared in a scatter diagram in Figure C-1. For Mitchell and Kammer No. 1, the calculated plume rises are in good agreement with the observations and the scatter of data points about the line of perfect correspondence does not appear to be systematic. Although the wind speed at stack height exceeded the exit velocity of the Mitchell stack during some of the trials, no exit-velocity (downwash) restrictions on plume rise are evident in the data. As previously noted, exit-velocity restrictions on plume rise were not expected because of the low Froude number (about 0.2) of the Mitchell stack during these trials. In every case, the plume rise calculated for Kammer No. 2 exceeds the "observed" plume rise. As explained above, this result was expected bacause of the interaction of this plume with the terrain at the distance of the aircraft measurements.

Axial Concentration

Table C-4 presents the calculated and observed axial SO_2 concentrations; the data points in Table C-4 are also shown in a scatter diagram in Figure C-2. Heights 1 and 2 in the table are the heights of the two highest measured concentrations and refer either to the two Kammer plumes individually, or to a single

TABLE C-3

CALCULATED AND OBSERVED PLUME RISES FOR THE
MITCHELL AND KAMMER POWER PLANTS

Trial No.	Mitchell Plume Rise (m)			Kammer No. 1 Plume Rise (m)			Kammer No. 2 Plume Rise*(m)		
	O	C	C/O	O	C	C/O	"O"	C	C/"O"
1	186	176	0.95	---	---	---	---	---	---
3	338	270	0.80	412	486	1.18	230	391	1.70
5	---	---	---	839	602	0.72	382	478	1.25
6	---	---	---	291	262	0.90	---	---	---
7	---	---	---	412	420	1.02	230	319	1.39
8	369	347	0.94	534	668	1.25	458	534	1.17
10	---	---	---	321	324	1.01	321	337	1.05
11	348	345	0.99	412	413	1.00	412	427	1.04
12	217	253	1.17	351	386	1.10	---	---	---
13	308	308	1.00	229	245	1.07	---	---	---
15	400	401	1.00	473	316	0.67	229	241	1.05
16	140	200	1.43	214	172	0.80	---	---	---
	Mean Ratio		1.04	Mean Ratio		0.97	Mean Ratio		1.24

O = Observed plume rise
C = Calculated plume rise
O/C = Ratio of calculated and observed plume rise

*See the discussion of plume rise

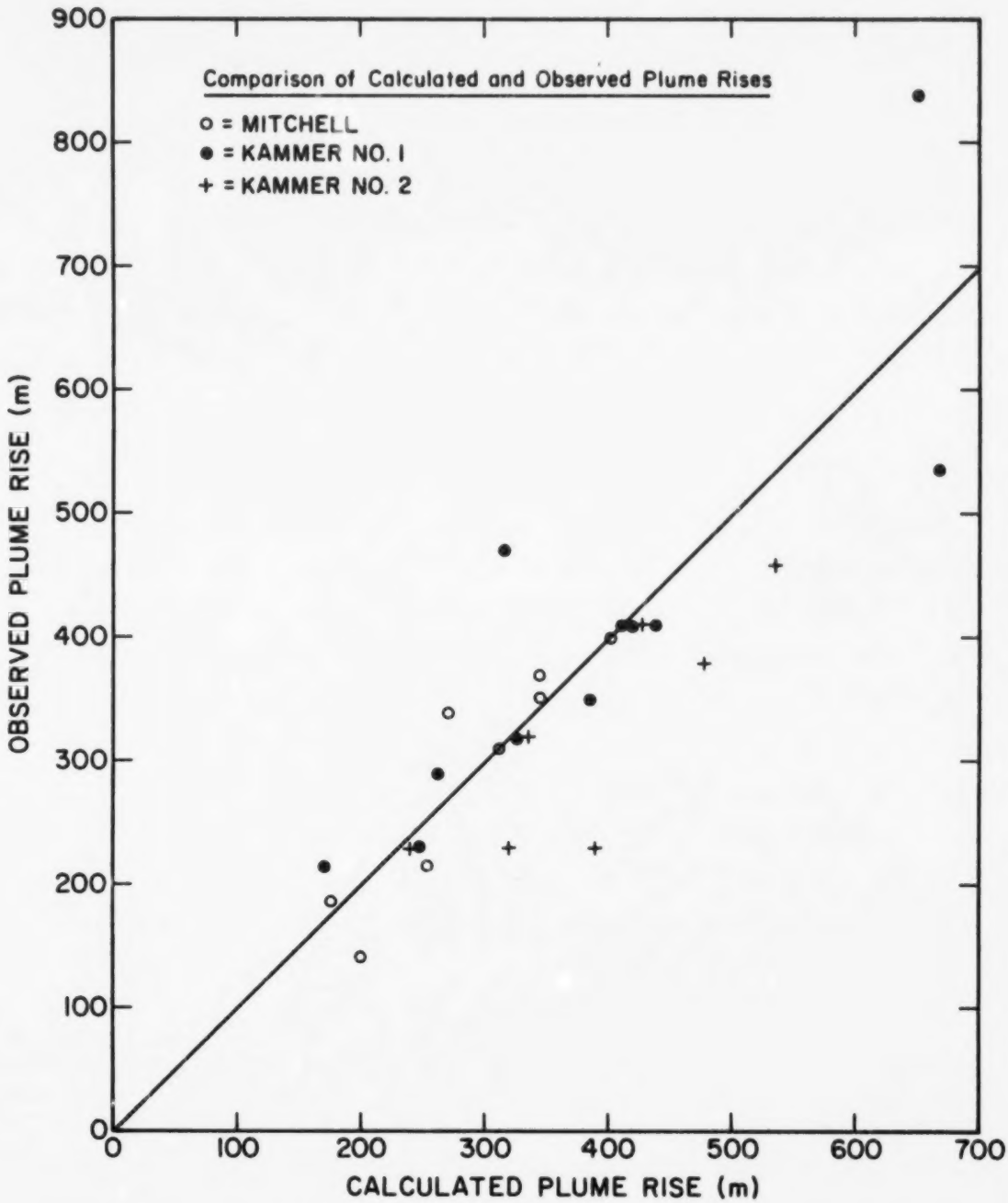

FIGURE C-1. Comparison of calculated and observed plume rises. The straight line is the line of perfect correspondence.

TABLE C-4

CALCULATED AND OBSERVED AXIAL SO_2 CONCENTRATIONS

Trial	Axial SO_2 Concentration (ppm)											
	Downwind Distance 1						Downwind Distance 2					
	Height 1			Height 2			Height 1			Height 2		
	O	C	C/O	O	C	C/O	O	C	C/O	O	C	C/O
3	0.71	0.67	0.94	0.68	0.75	1.10	0.26	0.17	0.65	0.28	0.17	0.61
5	0.25	0.33	1.32	---	---	---	---	---	---	---	---	---
6	0.99	1.48	1.49	---	---	---	0.60	0.52	0.87	---	---	---
7	0.51	0.53	1.04	---	---	---	---	---	---	---	---	---
12	0.50	0.62	1.24	1.17	1.47	1.26	---	---	---	---	---	---
13	1.86	2.35	1.26	---	---	---	0.87	0.65	0.75	1.15	0.69	0.60
	Mean Ratio		1.22	Mean Ratio		1.18	Mean Ratio		0.75	Mean Ratio		0.61

O = Observed concentration
C = Calculated concentration
O/C = Ratio of calculated and observed concentrations

TABLE C-5

MAXIMUM OBSERVED AND CALCULATED GROUND-LEVEL SO_2 CONCENTRATIONS

Trial	Terrain Height (m above MSL)	Observed Conc. (ppm)	Calculated Concentration (ppm)		$\frac{\text{Calculated Concentration}}{\text{Observed Concentration}}$	
			With terrain adjustments	Without terrain adjustments	With terrain adjustments	Without terrain adjustments
3	442	0.52	0.76	0.35	1.46	0.67
17	274	0.15	0.14	0.02	0.93	0.13
				Mean Ratio	1.20	0.40

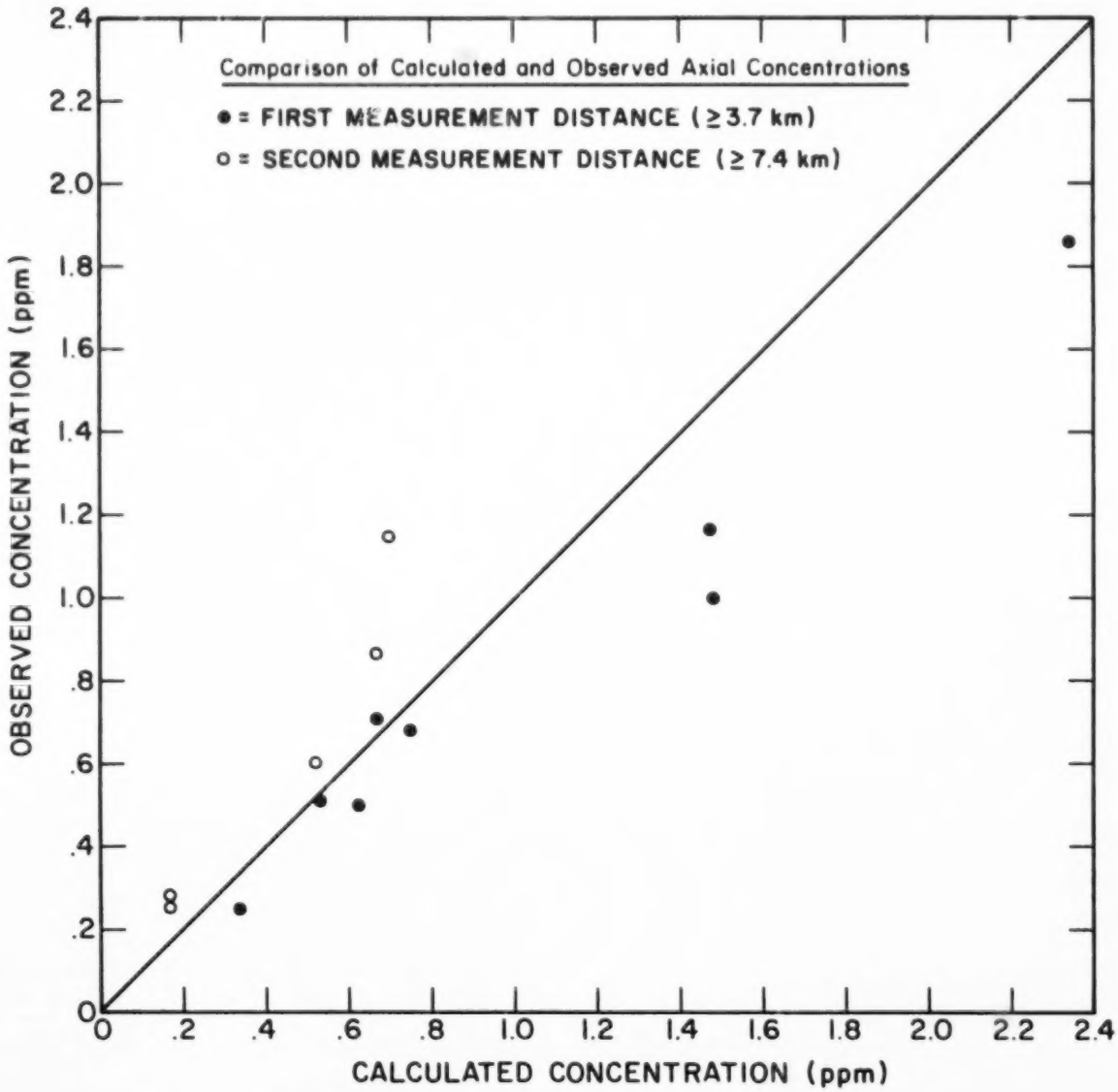

FIGURE C-2. Comparison of calculated and observed axial SO_2 concentrations. The straight line is the line of perfect correspondence.

merged Kammer plume and the Mitchell plume. Downwind Distance 1 in the table varies from about 3.7 to 11 kilometers and Downwind Distance 2 varies from about 7.4 to 18.5 kilometers. As discussed above, the heights of the two highest observed concentrations do not necessarily correspond to the actual plume stabilization heights because of the effects of reflection and interaction of superposed plumes. The calculated axial concentrations are the concentrations calculated by means of the short-term diffusion model equations at the heights of the highest concentrations measured by EMSL, using the Briggs plume rise formulas to obtain plume stabilization heights. The calculated axial concentrations thus include the effects of reflection and the combined contributions of the two Kammer plumes plus, where appropriate, the contribution of the Mitchell plume.

Table C-4 shows that the model estimates of axial concentrations are, on the average, approximately 21 percent larger than the observed axial concentrations at Downwind Distance 1. This could be due to the fact that the observed concentrations have not been adequately adjusted for the response time of the SO_2 instrument in the helicopter (see Johnson, et al., 1976). Also, the Mitchell plume bifurcated during several trials, and the model would be expected to overpredict axial concentrations within several kilometers of the stack under these conditions. At Downwind Distance 2, the calculated axial concentrations are all less than the observed concentrations. The fact that no SO_2 background is included in the calculated values partially accounts for this result. However, the possibility that the model overestimates lateral plume growth cannot be excluded.

Maximum Concentrations on Elevated Terrain

The Kammer plumes were observed intersecting nearby elevated terrain on at least two occasions. During Trial 3, the Kammer plumes were observed to be looping and intersecting a hill about 3.7 kilometers west of the Kammer Power Plant, and the EMSL helicopter made a single traverse through the plumes at

a height of about 15 meters above the surface. During Trial 17, the Kammer plumes were observed impacting on a hill about 2.8 kilometers northeast of the Kammer Power Plant, and the EMSL helicopter made 22 passes through the piumes at a height of 15 to 30 meters above ground level. Table C-5 lists the observed maximum SO_2 concentrations and the maximum 10-minute ground-level SO_2 concentrations calculated with and without the terrain-adjustment procedures described in Section A.5 of Appendix A. As noted above, the observed maximum SO_2 concentration for Trial 3 is based on a single pass through looping plumes. The observed maximum SO_2 concentration given in Table C-5 for Trial 17 is the average of the maximum SO_2 concentrations measured during the 22 traverses and thus should be more representative. Table C-5 shows that the best correspondence between the observed concentration and the 10-minute concentration calculated by including terrain effects occurs for Trial 17. If it is assumed that the plume axes are terrain following and thus no terrain adjustments are required, the calculated concentrations for both trials are significantly lower than the observed concentrations.

C.5 CONCLUSIONS

We conclude that the EMSL measurements support the short-term diffusion models and modeling procedures, including the terrain-adjustment procedures, used in this study. It should be noted that the long-term diffusion model used in this study, which includes the same assumptions about plume rise, plume growth and terrain effects, can be readily derived from the short-term model (for example, see Calder, 1971). We therefore conclude that the EMSL measurements also support the validity of the long-term model.